University of Technology, Sydney

Faculty of Engineering and Information Technology

Generation in Smart Cities: Building of Micro Scale Water Turbine for Rainfall

By

Jose Jaime Rodriguez

Student Number: 99214266

Project Number: A16-292

Major: Industrial Engineering

Supervisor: Dr. Huu Hao Ngo

A 12 Credit Point Project submitted in partial fulfilment of the requirement for the degree of the Degree of Bachelor of Engineering

Autumn 2016

Statement of originality

I confirm that I have read, understood and followed the guidelines for assignment submission.

I confirm that I have read, read understood and followed the advice in my subject outline about assessment requirements.

I understand that if this assignment is submitted after the due date it may incur a penalty for lateness unless I have previously had an extension of time approved and have attached the written confirmation of this extension.

Declaration of originality

The work contained in this assignment, other than that specifically attributed to another source, is that of the author(s) and has not been previously submitted for assessment. I understand that, should this declaration be found to be false, disciplinary action could be taken and penalties imposed in accordance with University policy and rules. In the statement below, I have indicated the extent to which I have collaborated with others, whom I have named.

Rodriguez, Jaime

Abstract

Generation in Smart Cities: Building of Micro Scale Water Turbine for Rainfall (12cp)

Jaime Rodriguez - A16-292

Supervisor : Dr. Huu Hao Ngo

Assessor : Dr.Wenshan Guo

Major: Industrial Engineering

In all the countries around the world, the concentration of population in urban areas is increasing, and so is the demand for energy. Given that fossil fuels still account for the largest part of the energy production to cover that demand and the environmental harm that this involves, it is necessary to start promoting initiatives to reduce this environmental impact. Since most of the population of the world lives in cities, implementing new ways of producing energy there would decrease the pressure that the environment is subject to due to the power demand.

The aim of this project is to design and build a micro-scale water turbine that harnesses the energy contained in the rainfall to charge a battery, providing a micro-generation system that could be used for distributed generation in cities. The completion of this project requires selecting and assembling the appropriate mechanical, electrical and electronic components, so that energy can be efficiently transformed by the system.

The micro hydropower system, as well as its individual components, undergo testing. Experiments with different load, flow and head conditions are conducted to see what effect they cause in the performance of the system.

Acknowledgement

I would like to thank several persons that have helped me throughout the process of undertaking this project.

In first place, I would like to thank my family and friends for all the support provided, especially Anika Sulkowski for her endless will to help me completing this project and Fareed Usmani for his advice not only about technical aspects, but also about the capstone subject itself.

Also, I would like to thank the staff from the Faculty of Engineering and IT workshop, especially Siegmund and Laurence, who advised and helped me designing and building the prototype.

Lastly, thanks to Dr. Huu Hao Ngo for accepting me as his capstone student and providing guidance and supervision.

Table of contents

Table of tables

Table of figures

CHAPTER 1

INTRODUCTION

1. Introduction

In the past decades, the lack of employment and development in rural environments in comparison to cities has led to a massive migration flow from rural to urban areas. According to data gathered by the Global Health Observatory from the World Health Organization, in 2014, 54% of the world population resided in urban areas, whereas in 1960, only 36% of the global population did.

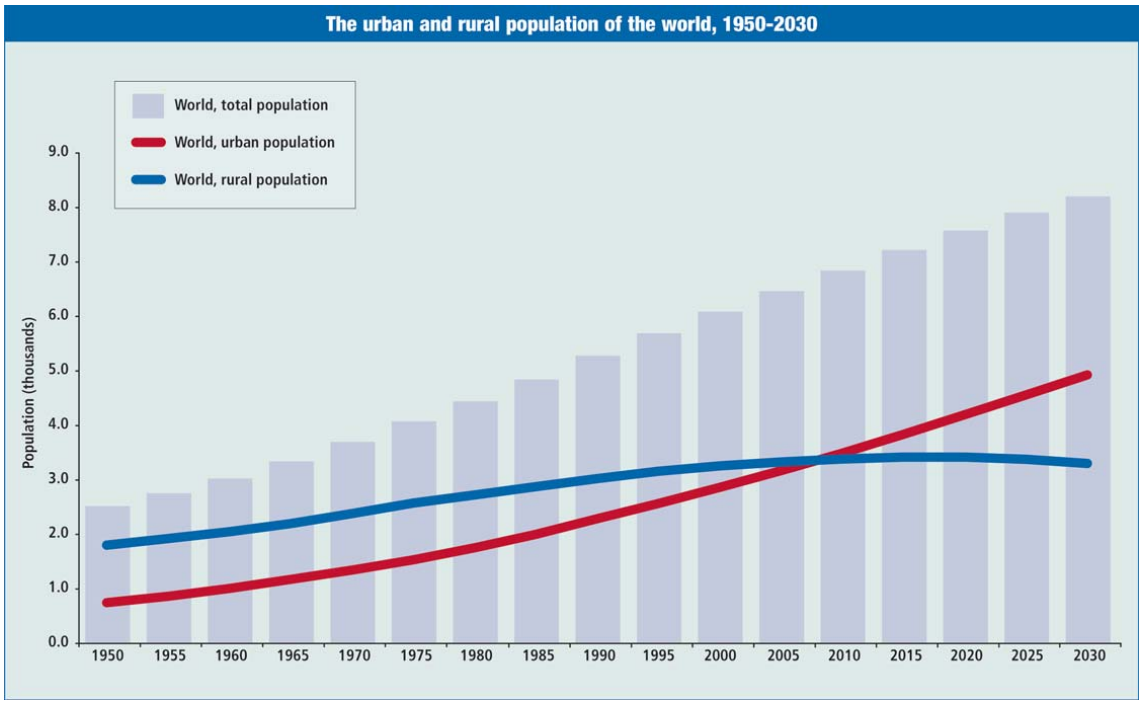

Figure 1: The urban and rural population of the world evolution (adapted from UN, 2005)

Cities are not expected to stop increasing in size and population, experts say. Moreover, the vast majority of the population, even in undeveloped countries, is expected to be living in cities by 2017 (World Health Organization, 2016).

This huge amount of people moving to urban areas presents many challenges that cities must face. Sometimes cities are not able to develop urban infrastructure and public services quickly enough to assist the needs of new incomers, such as transport, health, power lines, roads, etc., resulting in messy and tangled urban environments. Cities in developing countries, as Mexico DF or New Delhi, are currently undergoing this kind of issues.

In any case, the high concentration of population in cities brings along some other issues of major importance. Human activity takes resources from the environment and produces waste and pollution. The effect of human activity on the environment depends on many factors, however the environment will always get damaged to some extent. Especially in cities, the high

concentration of population yields constant, intense activity, that definitely affects the environment. Since cities are expected to keep increasing in size, the issue of their environmental impact should be thoughtfully addressed.

During recent years, many organizations and institutions have made growing efforts to inform world citizens about the ongoing climatic change issue and the consequences it could have not only in the environment, but also in economies and societies all around the world. The truth is that identifying and foreseeing all the risks and consequences that could derivate from the climatic change in the future is a daunting, difficult task. However, the initiative taken by these groups, added to the already visible evidence of climatic change in the world, such as the extinction of animal and vegetal species, the increment in the overall temperature of the world, or even the damage of the Great Barrier Reef in Australia, is turning up to be effective in rising people's environmental awareness as they realize that their day-to-day life could be dramatically affected. Although this awareness is still far from having reached enough importance to stop the climatic change by itself, it is expected to increase in coming years and become the main motivation source to counter climatic change at an individual scale.

When thinking of larger scale measures to fight climatic change, there are already some currently in place. Waste collecting, separating and recycling, enhanced energetic efficiency in buildings, more sensible usage of water resources are just some examples. It is in this context where the smart city concept arises as a great model that today's cities should move towards as one of its main aims is to lessen the harm that cities produce to the environment and, this way, decrease cities' contribution towards climatic change.

Smart city is a concept that represents the ideal city of tomorrow and involves many other concepts regarding smart power grids, multitude of sensing and metering devices, advanced IT technologies and renewable energy facilities among others. One of the main aspects that are part of a smart city is the so called distributed generation.

Distributed generation systems are those that satisfy all or part of the energetic needs in a demand point by producing electricity at the same point or close by.

The rated power of these sort of systems tends to be low and does not usually exceed tens of kilowatts, although they can reach a few hundreds of kilowatts in some particular cases. Therefore, distributed generation systems are also known as micro generation systems.

The production of energy in this way has several advantages compared to traditional generation and distribution systems (Sallam and Malik, 2011):

- Reduces the noxious emissions to the air as renewable energy sources are exploited
- Avoids the need of capital investments to develop distribution systems
- Greatly reduces the transmission and distribution losses since generation and demand points are spatially near to each other
- Provides an alternative power supply for applications that require uninterrupted energy supply, such as hospitals or banks
- Represents an electricity supply in remote locations that may be hard to be reached by the main power grid

Decentralized distributed generation (DDG) could also acquire a major role in achieving the universal electrification goal set for the year 2030. In opposition to most governments' plans to electrify remote rural areas just by expanding power grids and building more power plants, DDG could satisfy electrical demand in these places with small scale systems that would not only remove the dependence rural households have from the main power grid, but also would result in lower overall costs (Narula, K. et al., 2012)

By designing, building and testing a small scale water turbine that generates electricity by using the rainfall stored in a tank, which could be placed at the top of buildings or houses, this capstone project aims to provide a micro generation system that could be used for distributed generation applications. This device is not meant to generate huge amounts of energy, so it is a perfect example of a micro generation device.

CHAPTER 2

LITERATURE REVIEW

2. Literature review

Prior to undertaking the practical part of this capstone project, it is essential to go through the relevant theoretical aspects of the components that will be part of the final prototype.

2.1. Water turbine

2.1.1. Theoretical background

Water turbines are machines whose objective is to harness the energy contained in water to rotational kinetic energy. If attached to an electric generator, this rotational kinetic energy can be transformed into electrical energy. The water to be used with these devices is stored in a reservoir above the height where the turbine is placed. Since a difference of height exists between the water and the turbine, this provides the stored water with a surplus of potential energy respecting to the turbine's position. This potential energy is the one that later one is, partially, transformed into kinetic energy, which finally the water turbine converts into rotational kinetic energy.

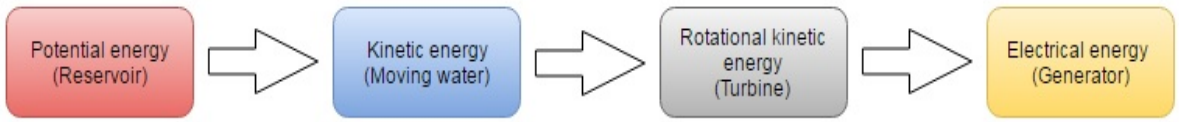

Figure 2: *Energy conversion diagram*

As water turbines have been used by mankind since a very long time ago, they have experienced great development and diversification. The range of currently available water turbines nowadays is very wide : Francis, Kaplan, Turgo, Pelton, waterwheels, crossflow turbines … In addition, some of them can have their shafts arranged either in vertical or horizontal position depending on what the requirements are.

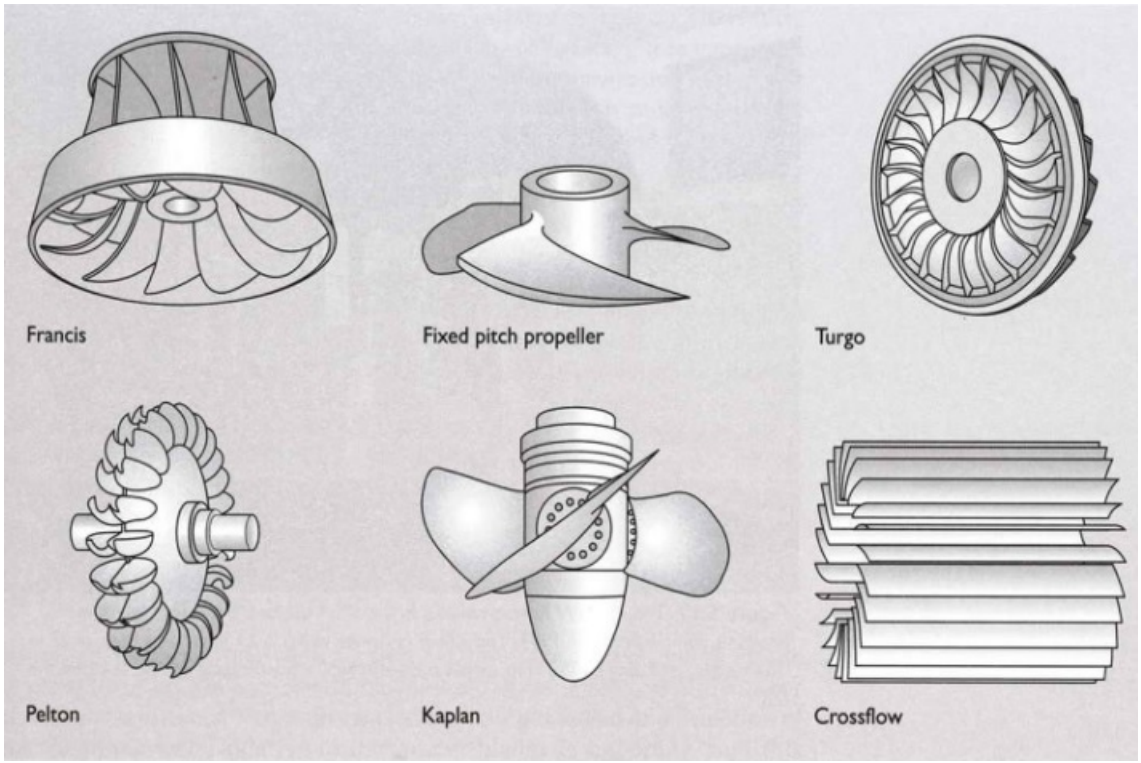

Figure 3: Types of turbine runner (modified from http://www.publicresearchinstitute.org/)

After reviewing the different types of turbines that are available nowadays, the Pelton turbine was found to be suitable for the purpose of the system. Pelton turbines allow working with a large range of heads, ranging from 20 to 1000 meters. It is important to note that lower flows (from 0.01 m^3/s to 0.5 m^3/s) are optimal when using Pelton turbines (Renewables First UK,2016).

The hydropower system is intended to be installed on top of buildings, whose height is usually around tens of meters. Moreover, the amount of water that can be collected at the top of those buildings cannot be expected to be very large, leading to reduced flow. Thus, the Pelton wheel turns out to be appropriate for this particular application.

The Pelton turbine falls into the so-called *impulse* turbines. The impulse, j, also known as quantity of motion, can be defined as :

$$j = m \cdot v$$

being m mass and v velocity.

The first derivative of the impulse is called the pulse force:

$$\frac{d(m \cdot v)}{dt} = \frac{dj}{dt} = F$$

The sum of all the forces that are present in a closed system equal zero, meaning that pulse forces are balanced with deflection and acceleration forces.

The peripheral flow reaching the jet drives the turbine's runner by producing a negative acceleration. This flow has a speed c_1. The power output of the turbine, P_T, can be calculated multiplying the rotational speed of the turbine runner, ω, and the produced torque in the turbine, M_T. P_T can be expressed too in terms of the flow rate Q, the peripheral velocity of the runner u, and the velocity components of the jet in the direction of u before it touches the bucket,c_1, and after it touches the bucket, c_2:

$$P_T = M_T \cdot \omega = \rho Q(c_1 - c_2)u$$

The turbine efficiency η_t is obtained by comparing the kinetic power of the jet,P_{jet}, and the power output that is produced at the shaft of the turbine, P_T:

$$\eta_t = \frac{P_T}{P_{jet}} = \frac{\rho Q(c_1 - c_2)u}{\frac{1}{2}\rho Q c_1^2}$$

It is useful to define a variable k that expresses the existing relationship between the peripheral velocity of the runner and the linear velocity of the jet before it reaches the runner:

$$k = \frac{u}{c_1}$$

The variable k becomes convenient since it can be used to determine the optimal rotational speed of the runner, ω_{opt}, obtained from the first derivative of the efficiency over k:

$$\frac{d\eta_t}{dk} = 0 \ \ (\omega = \omega_{opt})$$

When working with Pelton runners, it is important to describe the phenomena that are happening. If the vane moves towards the jet, the water increases its speed. In the opposite case, where the vane moves away from the jet, the water decreases its velocity. In case the vane is moving driven by the water at half its speed, (and assuming the friction can be disregarded), the water transfers all of its kinetic energy and just dribbles out of the moving vane.

Before reaching the runner, the water goes through the nozzle, which causes energy losses due to friction. Although with well designed nozzles with proper surfaces efficiencies between 0.96 and 0.99 can be reached, these losses should not be disregarded. Introducing the term φ_n allows to account for these losses, giving the jet velocity c_o:

$$c_o = \varphi_n\sqrt{2gH} = \varphi_n\sqrt{\frac{2p}{\rho}}$$

where H and p the pressure. The velocity of the jet when it touches the runner c_1 is assumed to be the same as the jet velocity at the noozle c_o.

The nozzle efficiency can be calculated as:

$$\varphi_n = \frac{\frac{1}{2}\rho Q c_1^2}{pQ} = \frac{\rho c_1^2}{2p}$$

If the deflection of the jet θ is assumed to be 165º, which is necessary to ensure that deflected water does not hit the following buckets, the power output of the Pelton turbine can be calculated as follows:

$$P_T = M_T \cdot \omega = F \cdot u = \rho Q(1 - cos\theta)(c_1 - u)u$$

and therefore, the efficiency of the Pelton turbine can be expressed as:

$$\eta_t = \frac{P_T}{P_{jet}} = \frac{\rho Q(1 - cos\theta)(c_1 - u)u}{\frac{1}{2}\rho Q c_1^2}$$

using the previously defined variable k:

$$\eta_t = \frac{P_T}{P_{jet}} = \frac{2(1 - cos\theta)(c_1 - u)u}{c_1^2}$$

$$\eta_t = \frac{P_T}{P_{jet}} = 2(1 - cos\theta)(1 - k)k$$

Once the first derivative of the efficiency is equaled to zero, it is simple to calculate the value of k for which the maximum efficiency is obtained:

$$k(\eta_{max}) = 0.5 = \frac{u}{c_1}$$

Thus, the maximum efficiency is obtained when the runner tip speed equals half the velocity of the jet. However, in real systems, the optimal value for k turns out to be between 0.45 and 0.49.

Theoretically, the maximum efficiency is:

$$\eta_{max} = \frac{1}{2}\varphi_n^2(1 - \varphi_b cos\beta_2)$$

which is the range of 0.95 provided that optimal nozzle efficiency is used. Pelton turbines can reach efficiencies as high as 88-91% when well designed, operating at 60-80% of full design flow.

When working with turbines, it is convenient to define how to calculate the speed of the jet c_1 and the speed of the turbine runner u at pitch circle diameter PCD:

$$c_1 = \frac{Q}{a_{jet}} = \frac{4Q}{\pi d_{jet}^2}$$

$$u = \omega \frac{PCD}{2}$$

The electrical energy output capacity of a turbine directly depends on its design and geometry. However, a water turbine is part of a system that contains water reservoirs and pipes to convey water turbine, among other elements. The configuration of this system determines the amount of power that can be extracted from water by its characteristics: net head, losses in pipes due to friction and geometry, etc (Unknown, 2016).

The hydropower that is available for a system, P_h, is given by the following formula:

$$P_h = \rho Q g H \qquad (W)$$

where:

ρ is the density of water (~ 1,000 kg/m^3 at 10° C; kg/m^3)

Q is the discharge of the scheme (m^3/s)

gH is the specific hydraulic energy, which is expressed as:

$$gH = \frac{1}{\rho}(p_1 - p_2) + \frac{1}{2}(c_1^2 - c_2^2) + (Z_1 - Z_2) \qquad (J/kg)$$

In the aforementioned equation, p represents the pressure, c represents the speed and Z represents the altitude with respect to a reference level. 1 and 2 are indices used to designate the entry and exit point of the turbine.

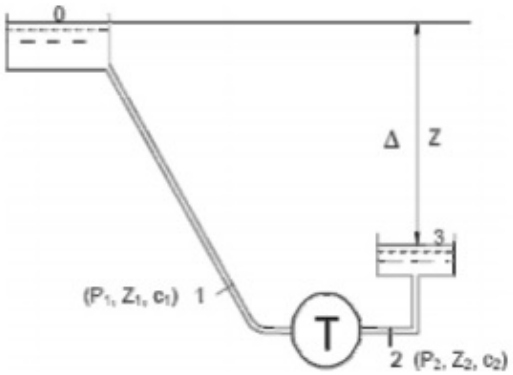

Figure 4: Typical scheme for an hydropower system (adapted from Sabonnadière, 2009)

Looking at Figure 4, it can be asserted that the pressure that levels Z_0 and Z_3 are submitted to is the atmospheric pressure. Also, the flow speed into these two basins is zero. Taking into account these considerations, the previous equation can be simplified as follows :

$$gH = g\Delta Z - gHr - \frac{c_2^2}{2} \quad (J/kg)$$

where:

ΔZ represents the difference in altitude between point 0 and point 3 (m)

gHr is a term that accounts for the losses produced in the pipe between levels 0 and 1, which are produced due to the friction and geometry of the pipe by elements such as narrowings or elbows. Empirical formulas or on the spot measurements can be used to determine this losses. It is important to note that these losses are proportional to the square of the flow speed in the pipe

$\frac{c_2^2}{2}$ is the kinetic energy that remains in the water flow after it has gone through the turbine and which cannot be recovered

The final electric output that the turbine will supply while functioning can be calculated from the hydropower P_h applying the efficiency of the different components that are part of the system as a whole :

$$P_e = P_h \cdot \eta_t \cdot \eta_m \cdot \eta_g \cdot \eta_d \quad (W)$$

In the equation above, P_e is the electric power output and P_h is the available hydropower for the given scheme. η_t accounts for the efficiency of the turbine (depends on the head and the discharge), η_m represents the efficiency of mechanical components such as bearings, gears, etc. (remains practically constant), η_g is the efficiency of the electric generator (varies with the turbine's mechanical output) and η_d represents the efficiency of the power electronics installed along with the system (Sabonnadière, 2009), .

2.1.2. Component review

2.1.2.1. Runner

The micro hydro system designed in this project harnesses the power through a Pelton water turbine. These kinds of turbines are the most suitable ones when working with low to high heads and low flows (Renewables First UK,2016)..

Since manufacturing the turbine and its spoons is a delicate and complex task that drastically affects the efficiency of the turbine, it was convenient to acquire it. Research was conducted and a variety of online manufacturers offering these items were found. Eventually, a manufacturer placed in Italy was found to provide a high quality turbine at a low cost that is designed to function in small scale hydro energy systems. The only drawback of this option was the long delivery time that the turbine took to arrive in Australia.

The reasons to choose this turbine over other turbines are the following:

- The efficiency that Pelton turbines reach decrease as the turbines grow in size. Therefore a small turbine like the chosen one was preferred.
- The reduced dimensions of this turbine allows the general system to remain small in size.

Figure 5: Selected Pelton turbine (modified from Ebay 2016)

As it can be seen in the pictures, the runner consists of a disk that has a number of spoons fixed at its circumference. In the center of the turbine there is a hole, which is intended to fit the shaft that will be used to attach the turbine to the generator. The three free small holes that are around the central hole aim to fit the screws that will fix the turbine and the shaft.

The main technical specifications have been gathered in the following table, as provided by the manufacturer:

Exterior diameter (mm)	117
Interior diameter (mm)	17
Pitch circle diameter (mm)	85
Number of spoons	16
Maximum pressure (bar)	15

Table 1: Turbine specifications (Ebay 2016)

2.1.2.2. Turbine shaft

Upon request, the same manufacturer that provided the turbine, accepted to make a shaft that would fit the purchased turbine. This turned out to be very helpful because, although the proposed shaft design was simple to manufacture with the proper equipment, these machines (lathe machines, drilling machines, etc.) have been really hard to find even in UTS and the access to them is very restricted to staff and highly trusted students.

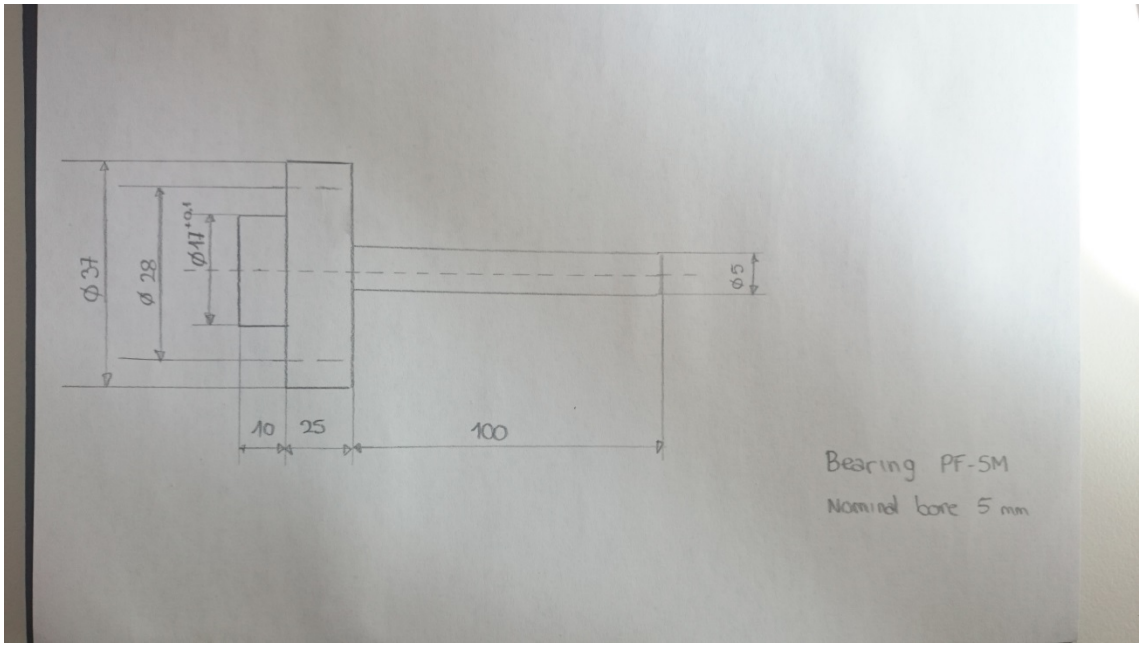

Figure 6: Proposed shaft design

Unfortunately, due to unknown circumstances, there was a misunderstanding with the manufacturer, and the shaft that was received highly differed from the one that was expected: it has a greater diameter than the design that was provided to the manufacturer, and it actually has a hole in the center of the shaft, which made it absolutely useless for the intended purpose at first.

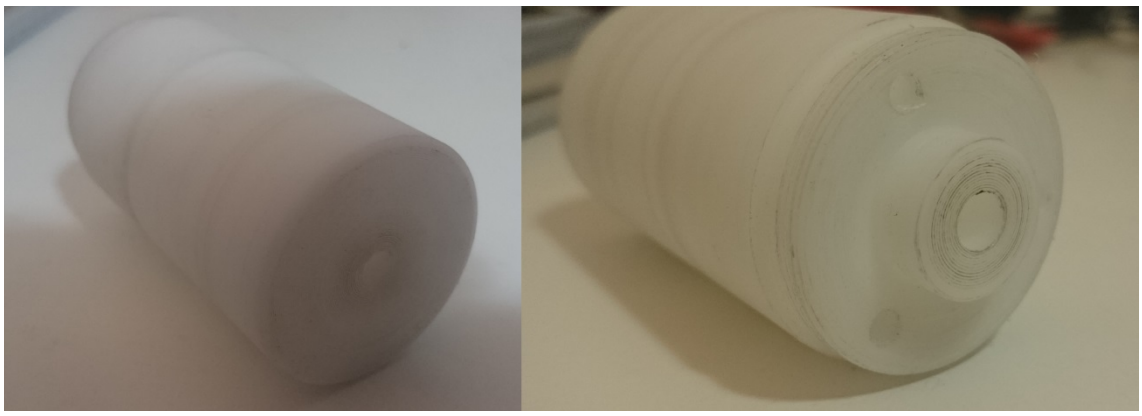

Figure 7: Received shaft

However, perpendicular to the axis of the shaft, there is a hole with a screw inside. This was basically the key reason why using this shaft instead of attempting to manufacture a new one with the available measures here was considered. By screwing this screw, it moves down the mentioned hole, so that a small rod able to fit in the inner hole of the shaft can be held.

Figure 8: Screw used to hold the inner shaft

This way, it is possible to have a turbine output shaft whose diameter is the same as specified in the original design, which was crucial to comply with the dimensions of the rest of components.

The preferred material for this rod would be some sort of metal, since it has to be resistant enough to stand the weight of the provided shaft and turbine. Metal retailers in the Inner Sydney area were contacted and, eventually a rod of correct dimensions was acquired at a very low cost. The outcome after assembling the metal rod and the shaft can be seen in the next figure:

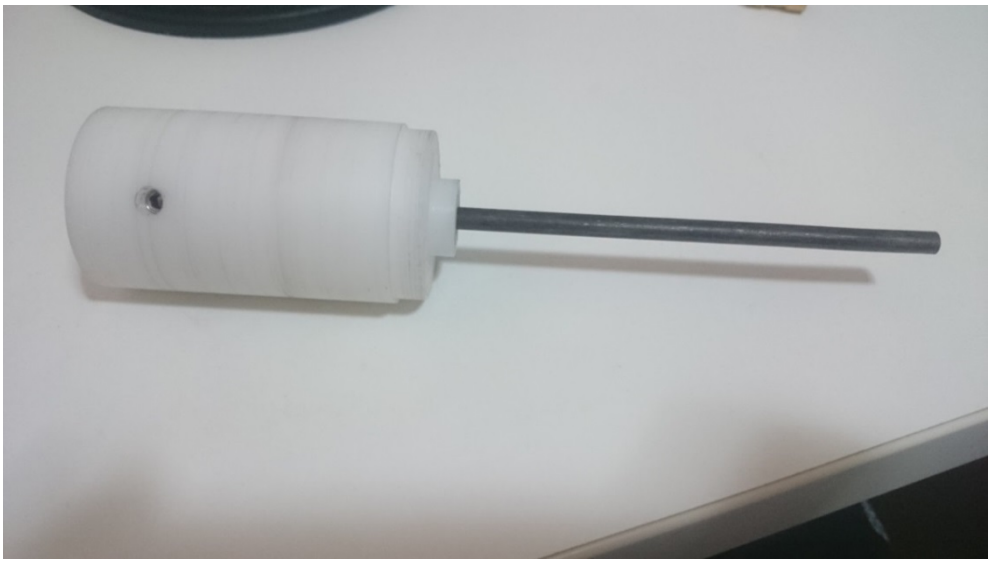

Figure 9: Rod and shaft assembled

Eventually, it was possible to access the FEIT workshop located in the basement of building 2 and make use of the power tools that are available there. Thanks to the very valuable assistance of the workshop staff, it was possible in the end not only to manufacture the shaft design that was originally proposed, but also to choose the material with which it was to be manufactured. The chosen material was aluminum, provided its several advantages. In first place, it is a resistant, yet light material which perfectly aligns with the preferred characteristics for the shaft. In second place, aluminum is a material that has higher corrosion resistance when compared to other materials, and this is a big advantage given that the shaft is intended to function in an environment where moisture will be almost permanently present.

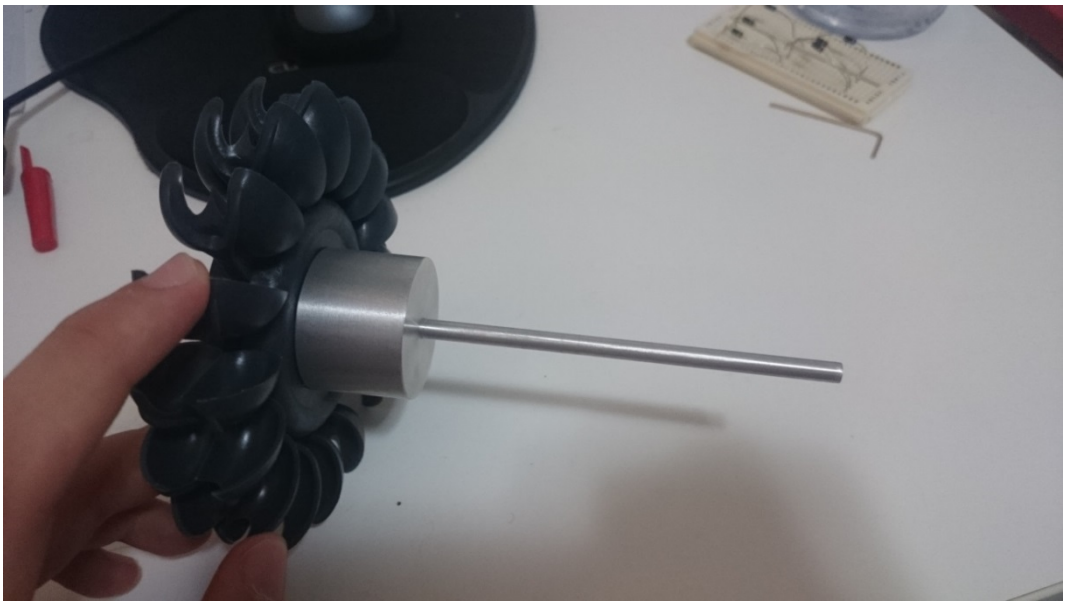

Figure 10: Final aluminum shaft

2.2. Electric generator

2.2.1. Theoretical background

In order to convert mechanical energy into electrical energy, the hydropower system to be built includes an electric generator. For this particular layout, the most suitable option is a 3-phase permanent magnet synchronous generator. The differentiating feature of this kind of generators is that they generate electricity whose frequency is proportional to the mechanical speed of the machine (Fitzgerald et al., 1992):

$$f = \frac{P}{2}\frac{n}{60} \qquad (Hz)$$

where f is the frequency of the voltage wave produced by the machine, P is the number of poles in the rotor, and n is the mechanical speed in revolutions per minute.

When analyzing a 3-phase synchronous generator it is convenient to focus only on one of the phases, as the analysis of the phenomena occurring in the chosen phase applies for the other phases too. The generated voltage will be influenced by the parameters that describe the machine : stator resistance, armature leakage reactance and reactance of armature reaction.

In phase 'a' voltage, $\widehat{V_a}$ (phasor), is:

$$\widehat{V_a} = \widehat{E_a} - jX_{al}\widehat{I_a} - jX_a\widehat{I_a} - R_a\widehat{I_a} \quad (V)$$

where $\widehat{E_a}$ is the stator induced voltage, $\widehat{I_a}$ is the phase 'a' current, X_{al} is the armature leakage reactance, X_a is the reactance of armature reaction and R_a is the stator resistance. The armature leakage reactance and the reactance of armature reaction can be added in a same term, called synchronous reactance :

$$X_s = X_a + X_{al}$$

Combining expressions the previous expressions, we obtain a formula that turns out very useful to model one of the phases of a 3-phase synchronous generator:

$$\widehat{V_a} = \widehat{E_a} - (R_a + jX_s)\widehat{I_a} \qquad (V)$$

The equivalent circuit that models one of the phases of the machine can be therefore represented as follows:

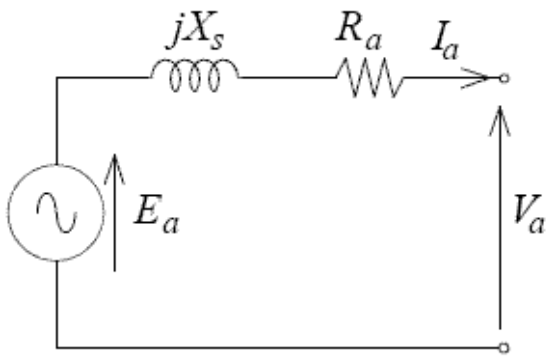

Figure 11: Equivalent circuit of 'a' phase (adapted from http://electrical-riddles.com/)

When looking at the machine as a whole, i.e. regarding all of the phases, they can be either star connected or triangle connected as shown in the following figure:

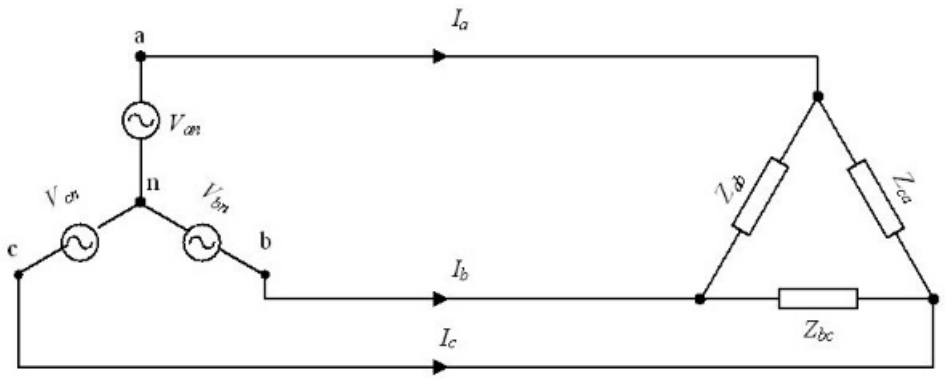

Figure 12: Possible connections between phases (adapted from http://www.intechopen.com/)

2.2.2. Component review

As previously mentioned, a 3-phase permanent magnet synchronous generator is implemented along with the system in order to generate an electric power output. The chosen generator was obtained from an online retailer after reviewing some other possible options at an affordable cost and can be seen in the following figure:

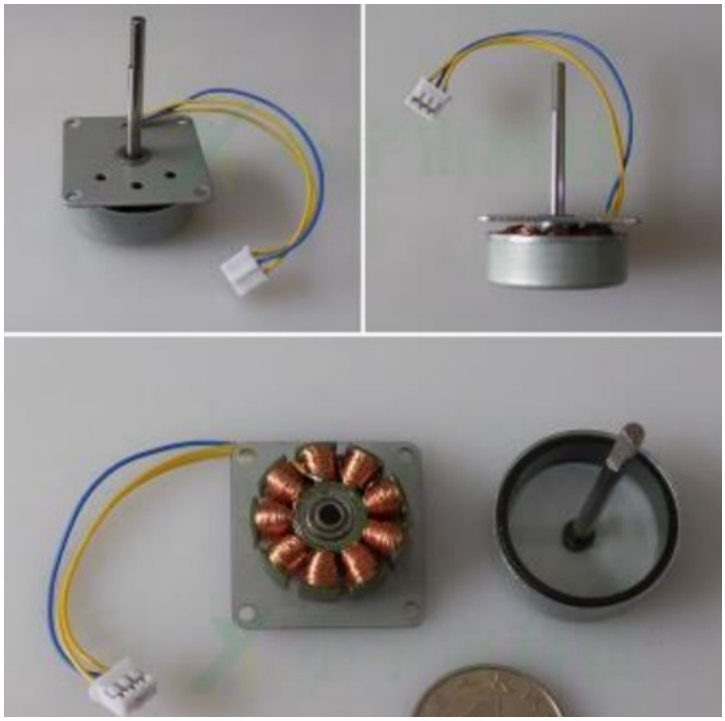

Figure 13: Electric generator used in the system (adapted from Ebay 2016)

The retailer provided information about dimensions and electrical characteristics, gathered in the following table:

Generator size (mm)	30x30x13.2
Rotor size (mm)	ϕ28.5x10
Stator size (mm)	30x30x11
Shaft size (mm)	ϕ3x31.5
Output voltage (V)	3 – 24
Output current (A)	0.01 – 1
Rated speed (rpm)	300-6000
Rated power (W)	0.5 – 12

Table 2: Electric generator characteristics (Ebay 2016)

The overall size and mass of the generator makes it suitable for a microgeneration system since it grants mobility and reduced dimensions to the general system. The electrical characteristics (output voltage, output current and rated power) seem to be able to fulfill the generation needs of the water turbine.

2.3. Rectifier

2.3.1. Theoretical background

The proposed hydropower system will include a rectifier whose aim is to transform the power output from the generator, which is provided in the form of a sine wave ac voltage, into dc electricity. A three-phase, full-bridge rectifier is a great option for the system, since they have lower ripple content in the waveforms and they are able to handle higher power (Mohan et al., 2003).

The rectifier is composed of six diodes, arranged as shown in the following figure:

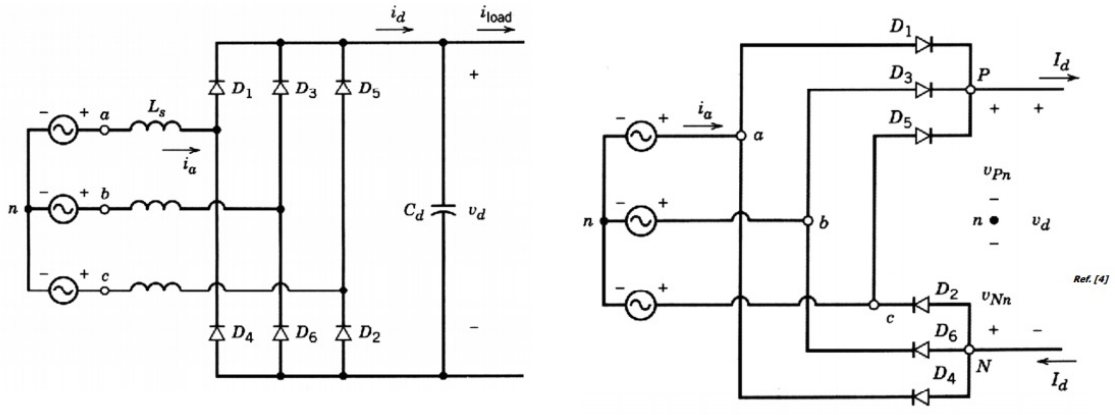

Figure 14: Three-phase, full-bridge rectifier (adapted from Mohan et al., 2003)

The function of this device is dominated by the switching principles of the diodes. In the top group (D_1, D_3 and D_5), the diode whose anode is submitted to the highest potential will switch on and start conducting, whereas the other two diodes will become reverse biased. Similarly, in the bottom group (D_4, D_6 and D_2), the conducting diode will be the one whose cathode is submitted to the lowest potential, and the other two diodes will become reverse biased.

The output of the rectifier is a six-pulse waveform, resulting from the different combinations of diodes conducting at each moment. The following figure illustrates both input and output in the rectifier:

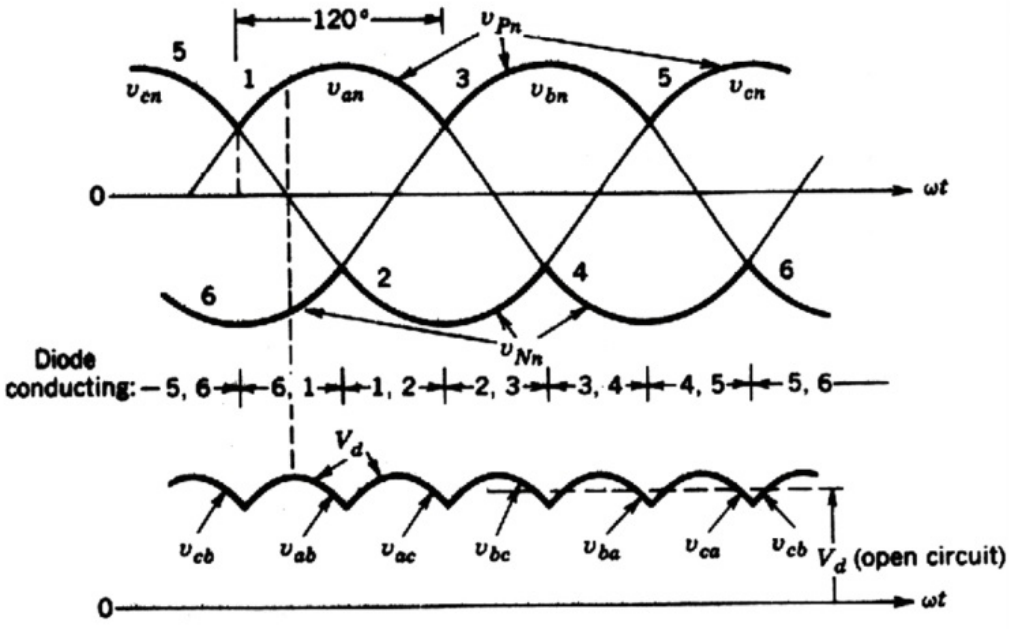

Figure 15: Rectifier input and ouput (adapted from Mohan et al., 2003)

The dc-side voltage, v_d, is:

$$v_d = v_{Pn} - v_{Nn} \quad (V)$$

being v_{Pn} the voltage at point P with respect to the voltage neutral point and v_{Nn} the voltage point at N with respect to the voltage neutral point, which can be obtained in terms of the input voltages of the three phases v_{an}, v_{bn} and v_{cn}.

The average value of the dc output voltage, V_d, assuming that L_s= 0, is:

$$V_d = 1.35\, V_{LL} \quad (V)$$

where V_{LL} is the rms value of the line-to-line voltages.

2.3.2. Component review

The rectifier was one of the easiest parts of the project to tackle. Within a short distance from UTS, there are plenty of stores that sell electronics products such as breadboards, diodes, switches, etc., so the acquisition was pretty simple to carry out.

A small breadboard able to fit in the turbine's stand and six diodes were purchased and assembled to implement the aforementioned rectifier, as shown in figure 7. The result can be seen in the figure below:

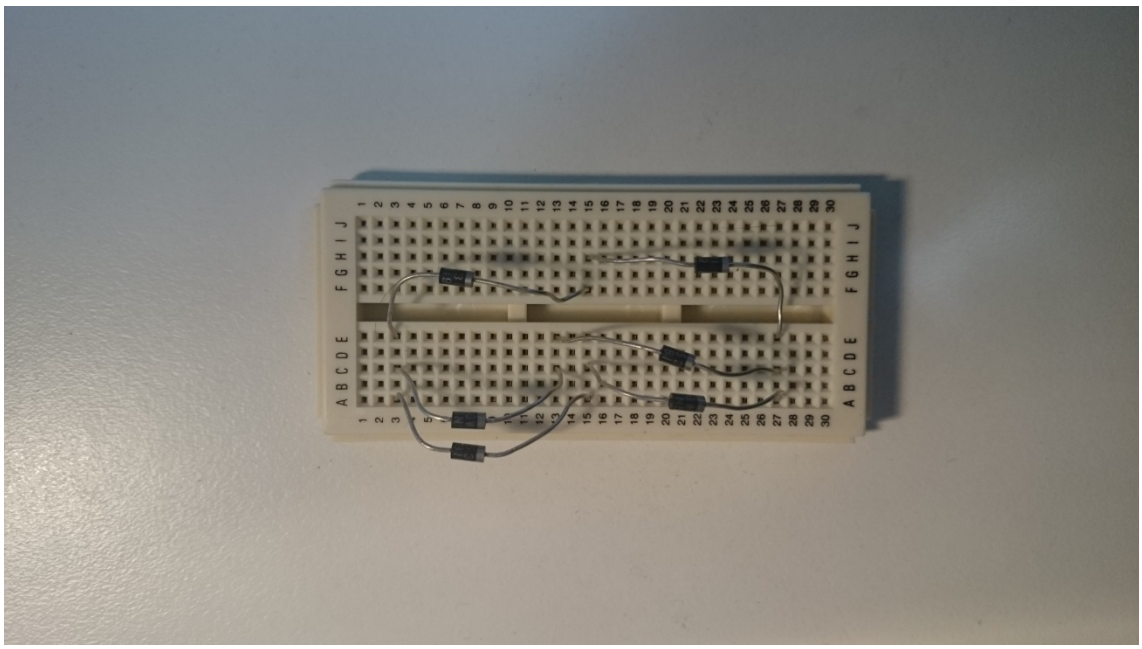

Figure 16: Rectifier

The range of diodes that are available in the market is massive, but since their price is not very high, it is possible to obtain diodes with high quality specifications at a low cost. For this case, diodes with the lowest possible voltage drop are preferred. Schottky diodes were found to be the ideal ones for this application, as they usually have smaller voltage drops and they have shorter switching times than regular diodes. Specifically, six Schottky 1N5819 diodes were implemented in the rectifier. The specification sheet of these diodes can be seen in datasheet section of references.

2.4. DC-DC Converter

2.4.1. Theoretical background

The system will feature a buck-boost dc-dc converter, which combines the functionalities of both buck and boost converters. This way, depending on the duty cycle, D,the output voltage can be amplified or reduced. The objective of implementing this device in the project is obtaining a regulated output voltage at a fixed value even though they input voltage may vary.

"The buck-boost converter is made by cascading the step-up (boost) and step-down (buck). In steady state, the voltage conversion ratio from input to output is the product of the conversion ratios of the two converters in cascade. However, for this to occur, the duty ratio on both converters must be the same" (Mohan et al., 2003).

.

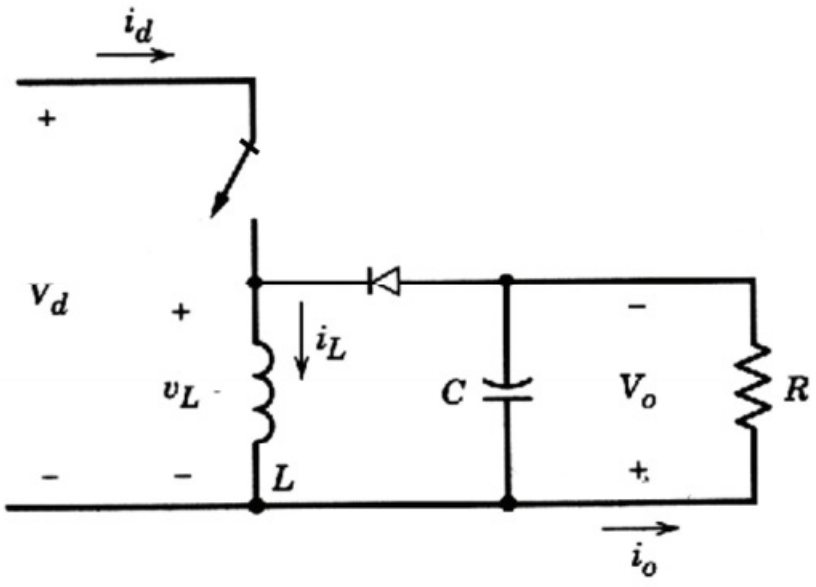

Figure 17: Buck-boost dc-dc converter (adapted from Mohan et al., 2003)

The following figure illustrates and explains how the converter functions. In the left part, the switch is on and the diode is reverse biased. The output side is isolated, so the load only receives power from the capacitator. In the right part of the figure, the switch is off and the diode is conducting. Therefore, the load receives power from the capacitator plus the power that the inductor has previously stored while the switch was on and that now is being transferred to the output. During this time, there is no energy supplied by the input.

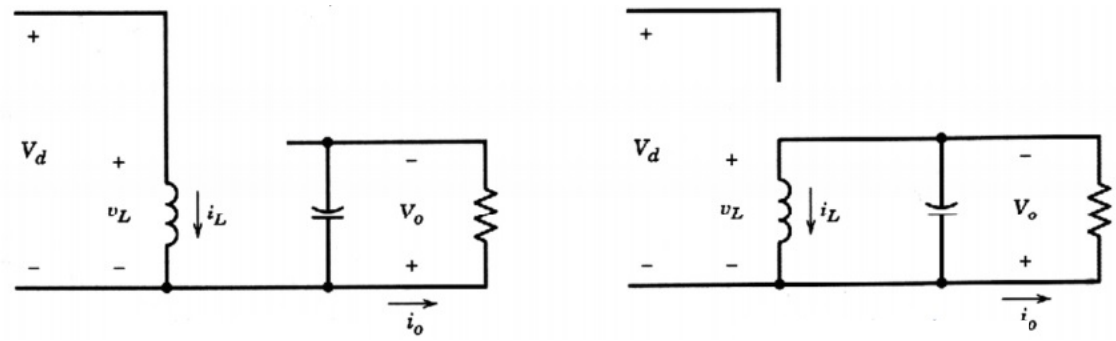

switch ON switch OFF

Figure 18: Function of the buck-boost converter (modified from Mohan et al., 2003)

The relationship between the input voltage, V_d, and the output voltage, V_o, can be expressed as follows:

$$V_o = D\frac{1}{1-D}V_d \qquad (V)$$

This relationship is dominated by the duty ratio, which can be expressed with the following formula:

$$D = \frac{t_{on}}{T_s}$$

t_{on} is the time of conduction of the switch, and T_s is the switching period. Analyzing equation 1.11, it can be asserted that:

- If $D < 0.5$, the converter will work as a buck converter
- If $D > 0.5$, the converter will work as a boost converter

It is important to note that the capacitator present in the converter's scheme is assumed to be large enough to allow an almost constant output voltage $v_o \cong V_o$.

2.4.2. Component review

In order to maintain a constant DC voltage in the output of the system, two different voltage regulators were considered from among all the available ones in the market considering the electrical characteristics of the final prototype.

The first of them is the 7805, and the second one is the LM2940CT-5. Both of them are designed to provide 5 V and 1 A as maximum in the output of the system. The LM2940CT-5 is slightly more expensive than the 7805, although after inspecting the datasheet of both components, it was found out that the LM2940CT-5 has a maximum dropout voltage of 1 V, whereas the 7805 has a dropout voltage of 2 V. For this application, the voltage regulator with the lowest dropout voltage is preferred because it requires a lower voltage to correctly function. Therefore, the LM2940CT-5 was chosen since the price difference was small enough to disregard it.

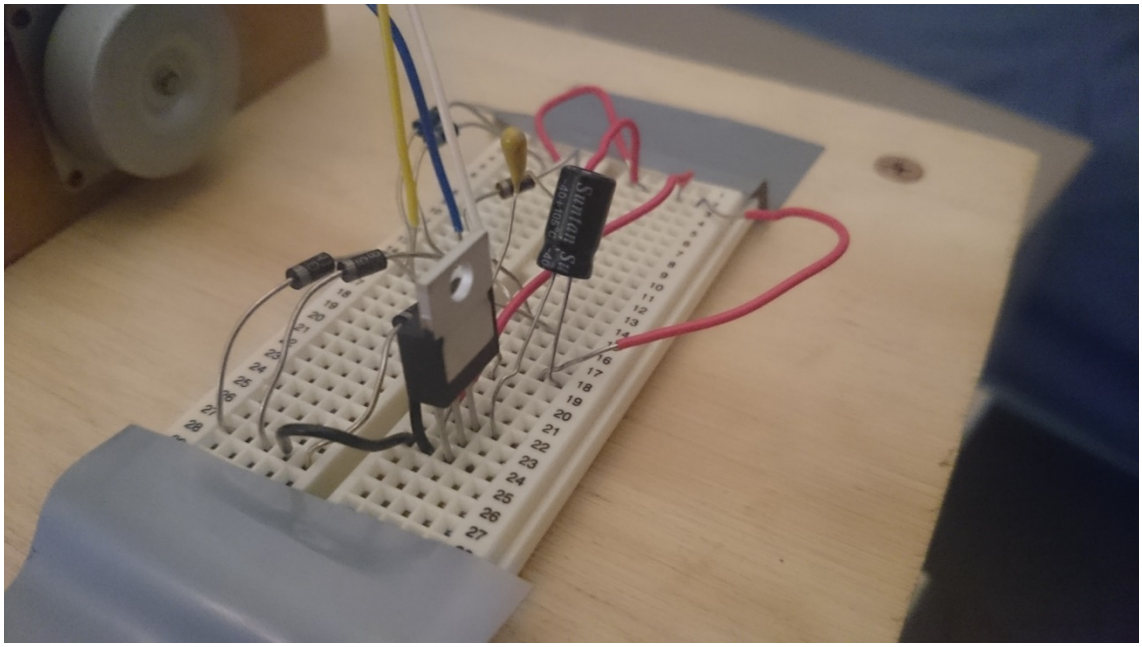

Figure 19: Voltage regulator and capacitator used to regulate voltage

The chosen voltage regulator can be seen in the figure above. The black capacitator is a capacitator that must be used to ensure that the voltage levels in the output are stable. According to the chosen regulator's datasheet, this capacitator must have a capacitance of 22 μF.

2.5. Mechanical components

In order to complete the assembly of all the parts of the prototype, some ancillary mechanical components were needed. An Australian retailer was found able to provide the proper parts after

conducting some research, thus being the order placed shortly after the dimensions for the mentioned parts were determined. Note that these dimensions were mainly determined by the size of the generator shaft, which has 3 mm in diameter.

2.5.1. Shaft coupling

The first issue to address was how to attach the generator shat and the turbine shaft, so that mechanical power can be transferred from the turbine to the generator in an efficient way. Exactly as happened with diodes, the amount of solutions for this matter that can be found in the market is huge, and so is the price range. When narrowing down the search to the least expensive components, rigid shaft couplings seemed to be the most suitable option as they are easy to install an efficient when it comes to transfer power in low power applications. They are offered either in plastic or metal materials, but metal was preferred due to its higher durability. Moreover, brass was offered as a material. This fact is of great importance, since it removes any problems that corrosion may cause since brass is a material that is highly corrosion-resistant. After considering all these factors, the part in the following picture was ordered:

Figure 20: Brass rigid coupling shaft, model CP-030-050-09-R-B

As it can be seen in the picture, the part basically consists of a brass tube with two bores of different size, plus two little screws in perpendicular position to both bores. These little screws can be screwed down their bores to hold the shafts inside the coupling and thus ensuring that

power is efficiently transferred. As previously mentioned, the size of this part was absolutely dependent on the diameter of the output shaft of the generator, which is 3 mm. Once the diameter of the first bore was specified, there were only a few diameter options for the other bore, ranging from 4 to 6 mm. The 5 mm option was chosen, which eventually determined the diameter of the turbine shaft.

2.5.2. Bearing

Apart from that, a bearing was necessary to hold the turbine shaft onto the stand. Again, the offer of components of this type that are available is very large. However, since this is an element that can have a remarkable impact on the overall efficiency of the system, bearing with reduced losses due to friction such as balls bearings were preferred. The same online retailer from whom the shat coupling was ordered offered a very interesting option that would save some work in the future: a bearing that was already placed inside a housing, with both components fitting perfectly. This bundle was offered at an affordable cost and it turned out very convenient as no further housing was needed to be made for the bearing. The ordered part can be seen in the following figure:

Figure 21: Housing and bearing used in the prototype, model PF-5M

When deciding the adequate diameter for the bearing, it was necessary to keep in mind that this bearing's aim is to support the shaft of the turbine. Nevertheless, the diameter of this shaft was

already determined by the bore diameter of the shaft coupling. Therefore, the diameter of the ordered bearing had to be 5 mm.

2.6. Stand

Once all the components were available, it was necessary to assemble all of them together and build a structure able to hold all of them. This structure was decided to be made out of wood, joint together by suing wood screws. The reason why wood was chosen is because is double. On one hand, it is a material that does not deteriorate quickly when exposed to water and moisture, and this resistance is even higher if the wood receives a varnish treatment. On the other hand, performing operations like drilling and cutting is extremely easy when working with wood, reducing the effort needed to build the stand that is meant to hold the system together.

The stand is basically a table-like structure, where the components were either nailed or glued. To mount the generator, a small vertical stand was cut and nailed to the main stand. Then the stator of the generator was glued to this stand, as it can be seen in the following figure:

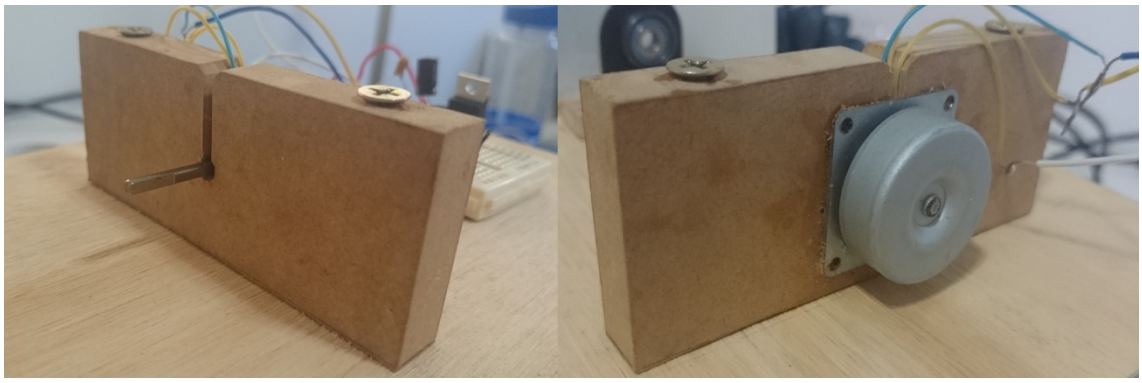

Figure 22: Stand for the generator

A small opening was made in this stand in order to make some room for the generator output cables, so that they were not forced against the stand, which could eventually unstick the stator from the stand.

After the generator was mounted, it was necessary to place the bearing on a small platform to ensure that the shafts of the generator and the water turbine were correctly aligned. This small wood piece can be seen in the following picture:

Figure 23: Stand for the bearing

2.7. Final build

The following figures show how the final prototype looked like once all the components were assembled. At this final assembling stage, a plastic case was added to the prototype to prevent water from splashing, which would not only damage the electronics of the prototype but also the metallic parts.

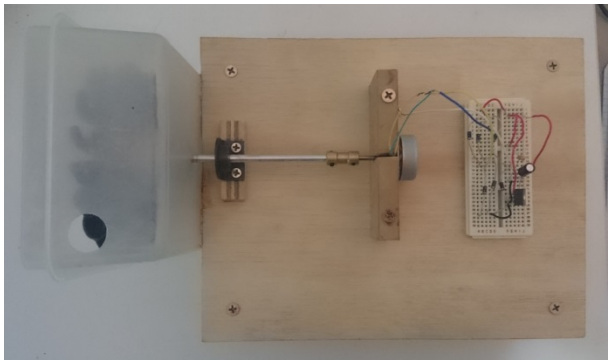

Figure 24: Upper view of the prototype

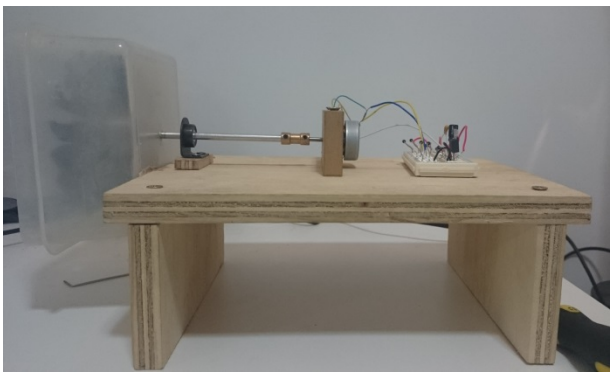

Figure 25: Side view of the prototype

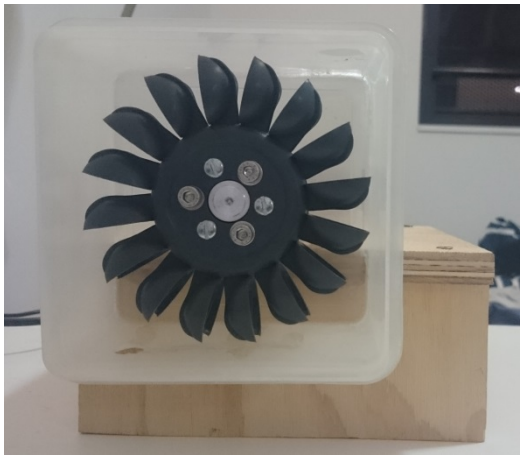

Figure 26: Turbine's side view of the prototype

The final configuration of the breadboard, including the full bridge 3 phase rectifier and the voltage regulator circuit, is shown in the following figure:

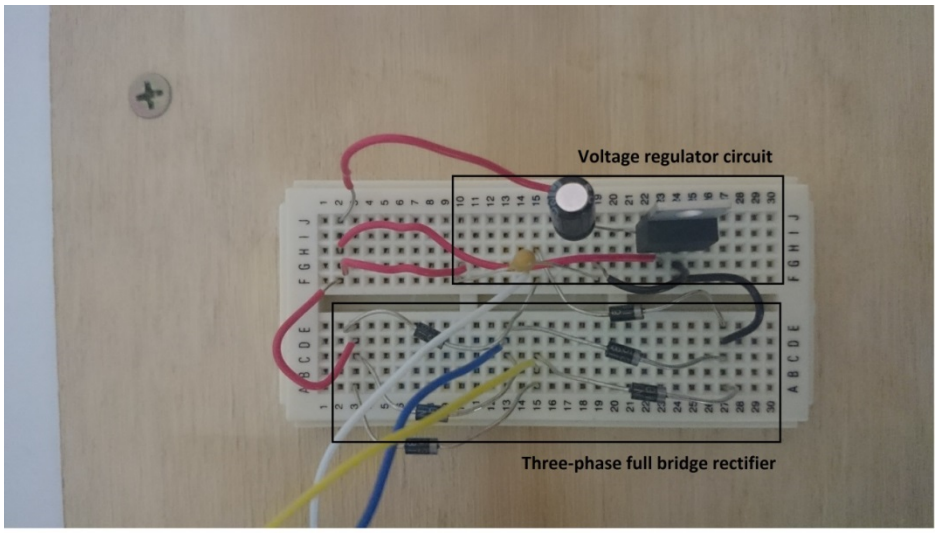

Figure 27: Final configuration of the electronic components on the breadboard

CHAPTER 3

EXPERIMENTAL INVESTIGATION

3. Experimental investigation

3.1. Electric generator testing

3.1.1. Number of poles test

One of the important parameters of the machine, the number of poles, was not provided by the manufacturer. Since this is a characteristic of major importance for the project, the rotor was separated from the stator and a simple test was conducted to find out the amount of poles. A metallic screw was moved all along the circumference of the permanent magnet rotor, and the number of times it was stopped due to magnetic attraction was recorded. The test yielded that this electric generator has 12 poles.

Figure 28: Test conducted to find out the number of poles

3.1.2. Resistance and inductance

Information regarding the resistance and inductance of the 3-phase synchronous generator was not provided either by the retailer. Again, these are parameters of high importance as no electrical analysis of the machine can be undertaken if they are unknown. Separate tests have been conducted to determine both resistance and inductance of the machine. It is important to keep in mind that we are working with a 3-phase machine, and therefore resistance and inductance must be measured from line to line. Thus, 3 tests were conducted for resistance, and 3 other tests were conducted for inductance.

Two of the three cables that the generator has are yellow, which could lead to confusions while undertaking the resistance and inductance tests. To distinguish one cable from another and solve this issue, one of the yellow phase cables was colored black. By coloring this cable in black, the color code of the cables also got to comply with Australian standards.

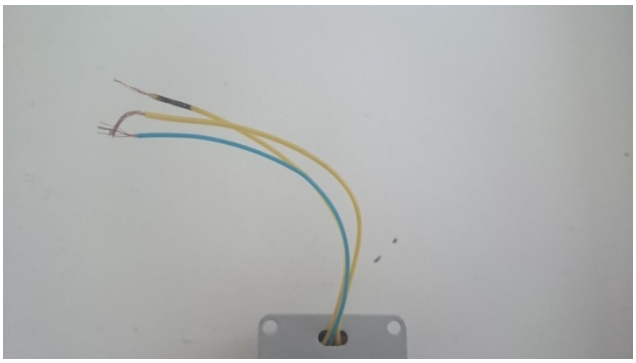

Figure 29: The three output wires of the generator

The equipment used to carry out the resistance tests was a multimeter. For further information about the multimeter, refer to appendix A. The results are displayed in the following table:

Phase	*Line to line resistance (Ω)*
Yellow to black	35.6
Yellow to blue	35.6
Black to blue	35.5
Selected value	35.6

Table 3: Generator resistance test values

In order to measure the inductance values, a “Vichy DM4070” LRC meter was employed. The results are displayed in the following table:

Phase	*Line to line inductance (mH)*
Yellow to black	15.5
Yellow to blue	19.7
Black to blue	15.5
Selected value	19.7

Table 4: Generator inductance test values

The selected values are the ones that will be used to model the generator for circuit representations and possible simulations. Since these values are measured from line to line, the values per phase are as follow:

Resistance (Ω)	17.8
Inductance (mH)	9.85

Table 5: Resistance and inductance values per phase

When looking at the obtained values, it can be noticed that the internal per phase resistance of the generator seems to be higher than what could be expected for a generator this size. To discard possible errors while carrying out the tests, the resistance value was rechecked by undertaking another test. With an ancillary generator, currents of small magnitude were passed through the wires of the generator, and the voltage drops were recorded. The resistance values obtained using this method were very similar to the ones obtained using the multimeter, thus being the original multimeter results correct.

Once the parameters of the machine are known, the single phase circuit diagram of one of the phases of the generator can be elaborated. The following figure shows the equivalent circuit for 'a' phase:

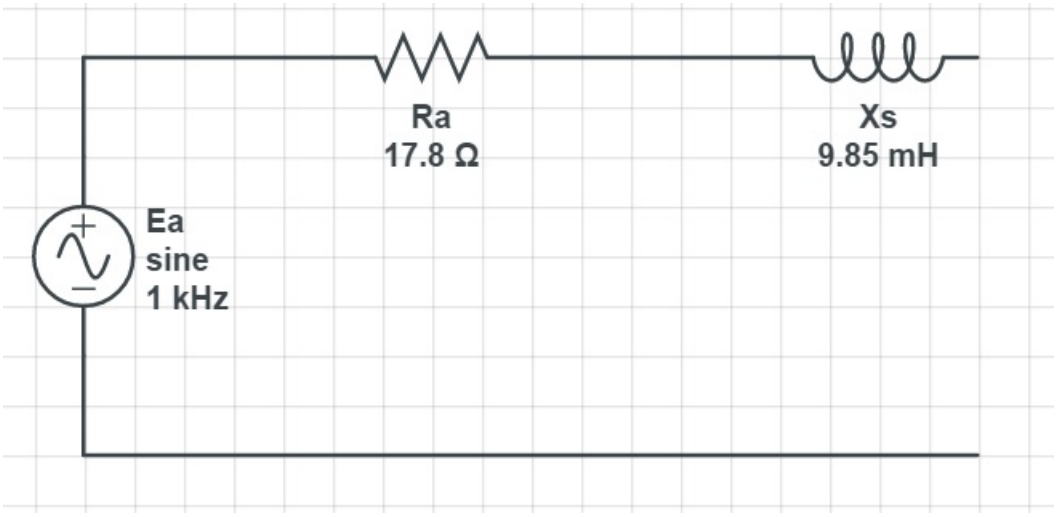

Figure 30: Equivalent circuit of 'a' phase

3.1.3. Voltage measurement

Before undertaking the assembly of all the components integrating the system, it seemed interesting to analyze the behavior of the electric generator with some simple tests. Specifically, tests to measure the line to line output voltage that the generator is able to produce with no load were conducted.

In these tests, the rotational speed that could be manually generated in the generator did not seem high enough to observe how the generator will behave when it is functioning together with the rest of the system. In consequence, an electric drill machine was used to obtain rotational speeds that better represent the future functioning conditions of the system. The drill machine allows varying the speed at which it spins, giving the opportunity to perform tests at different rotational speeds with the generator. To obtain representative information on what the voltage output of the generator will be when assembled with the rest of components, it was tested in three different conditions by putting the drill on minimum, medium, and maximum rotational speed.

While conducting the tests, it was convenient to make sure that the shaft of the generator was tightly attached to the shaft of the drill to avoid slipping. Also, it was necessary to firmly hold the stator of the generator to ensure that it does not rotate along with the rotor. The set up used to carry out the tests can be seen in the following figure:

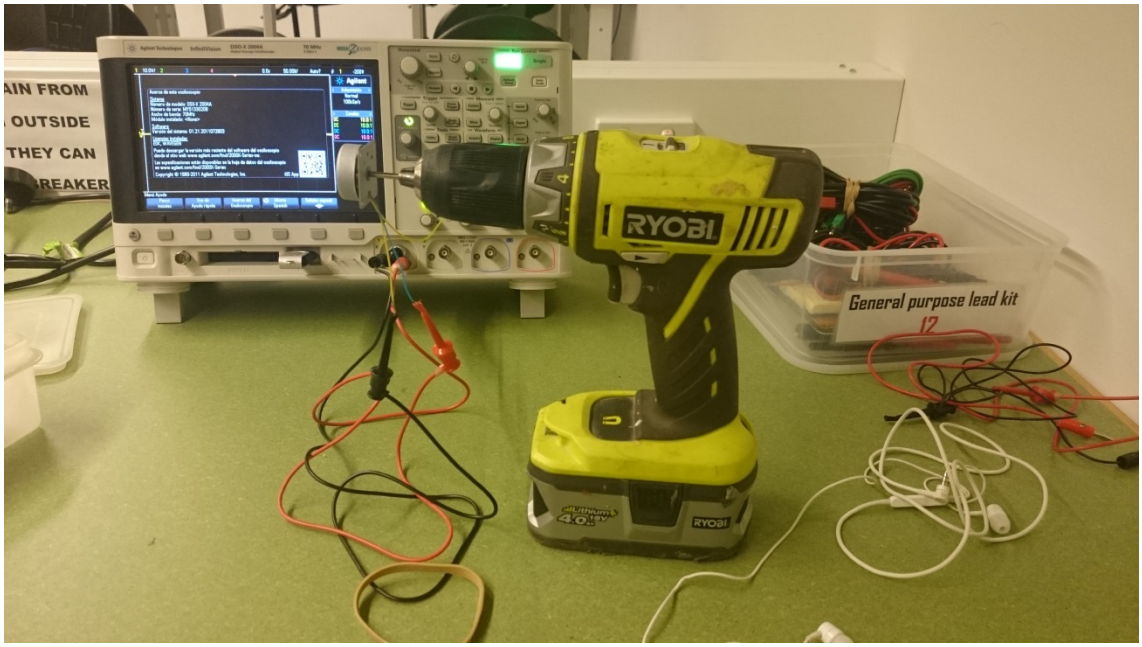

Figure 31: Voltage output test set up

To display and analyze the waveforms of the voltage that the generator was producing, one of the oscilloscopes available at the workshops in building 11 was used. Refer to the appendices for further information about the oscilloscope used.

3.1.3.1. Minimum speed test

In this test, the drill was rotated at its minimum speed. The outcomes of the test are shown in the following figure:

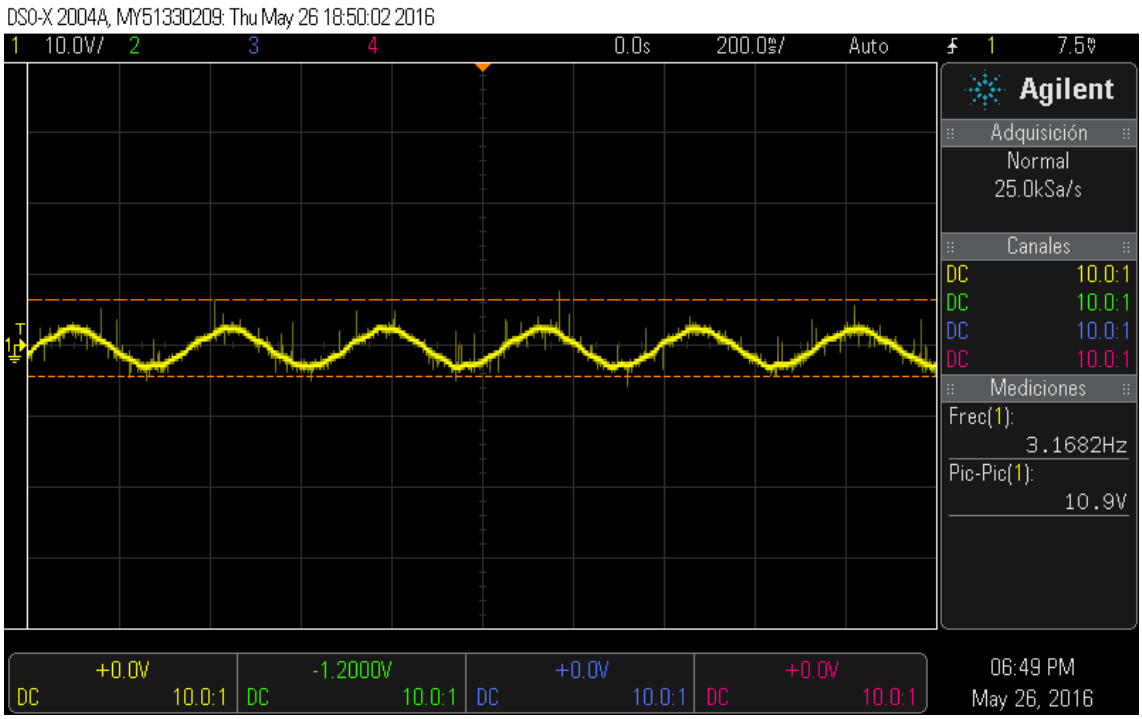

Figure 32: Snapshot of the minimum speed test

As it can be seen in the figure, the frequency is 3.17 Hz and the peak-to-peak voltage is 10.9 V.

Using the expression shown below and knowing that the number of poles of the generator is 12, it is possible to calculate the rotational speed of the machine:

$$f = \frac{P}{2}\frac{n}{60}$$

$$n = \frac{2 \cdot 60 \cdot f}{P} = \frac{2 \cdot 60 \cdot 3.17}{12} = 31.7\ rpm = 3.92\ rad/s$$

3.1.3.2. Medium speed test

In this test, the drill was rotated at medium speed. The outcomes of the test are shown in the following figure:

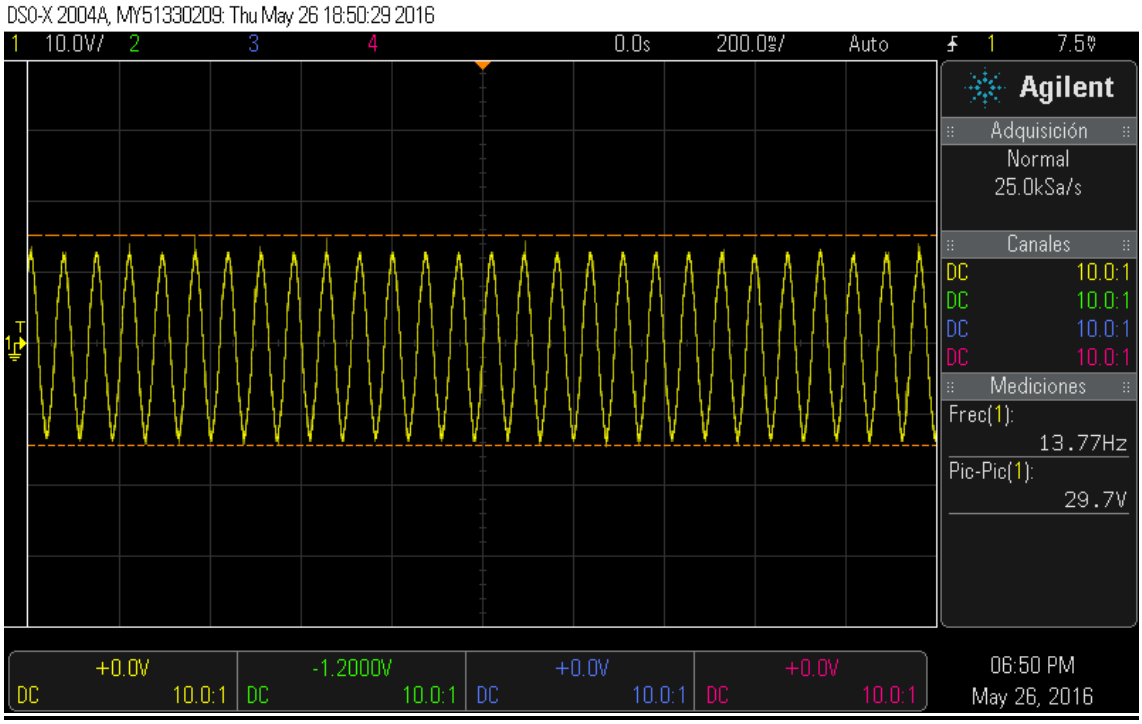

Figure 33: Snapshot of the medium speed test

As it can be seen in the figure, the frequency is 13.77 Hz and the peak-to-peak voltage is 29.7V.

Using the expression shown below and knowing that the number of poles of the generator is 12, it is possible to calculate the rotational speed of the machine:

$$f = \frac{P}{2}\frac{n}{60}$$

$$n = \frac{2 \cdot 60 \cdot f}{P} = \frac{2 \cdot 60 \cdot 13.77}{12} = 137.7\ rpm = 14.42\frac{rad}{s}$$

3.1.3.3. Maximum speed test

In this test, the drill was rotated at its maximum speed. The outcomes of the test are shown in the following figure:

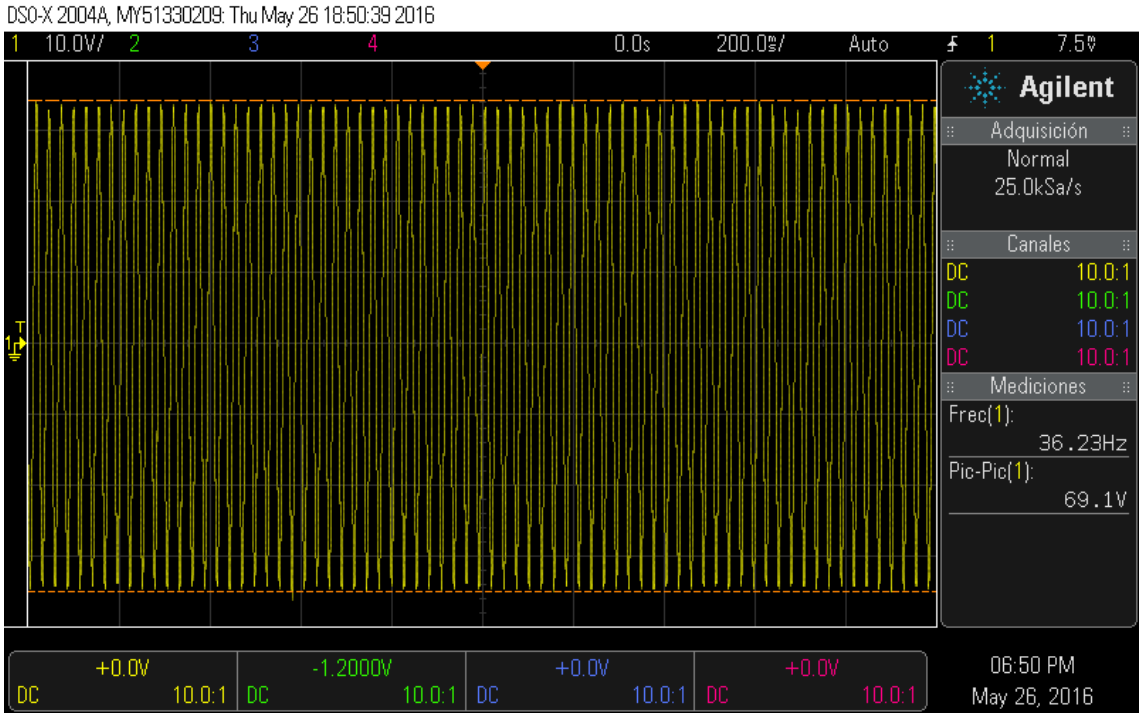

Figure 34: Snapshot of the maximum speed test

As it can be seen in the figure, the frequency is 36.23 Hz and the peak-to-peak voltage is 69.1 V.

Using the expression shown below and knowing that the number of poles of the generator is 12, it is possible to calculate the rotational speed of the machine:

$$f = \frac{P}{2}\frac{n}{60}$$

$$n = \frac{2 \cdot 60 \cdot f}{P} = \frac{2 \cdot 60 \cdot 36.23}{12} = 362.3\ rpm = 37.94\ rad/s$$

3.1.4. Back EMF constant

The back EMF constant is an interesting parameter of a permanent magnet machine that relates the voltage output and the rotational speed of the machine. It can be calculated with the following formula:

$$k_e = \frac{V_{pk}}{\sqrt{3}\omega_e} \qquad (\frac{V \cdot s}{rad})$$

being V_{pk} the line to line peak voltage produced by the generator and ω_e is the electrical angular frequency of the generator (Novotny and Lipo, 1996). The utility of this constant lies in the possibility of using it to calculate an estimate of the peak voltage that will be produced when the generator is rotating at a given speed.

The maximum speed test will used as reference to obtain the value of this constant:

$$k_e = \frac{V_{pk}}{\sqrt{3}\omega_e} \qquad (\frac{V \cdot s}{rad})$$

$$k_e = \frac{61.9}{\sqrt{3} \cdot 2\pi \cdot 36.23} = 0.157 \qquad (\frac{V \cdot s}{rad})$$

3.2. Rectifier testing

The rectifier was also tested before implementing the final design, and the results are shown in the following picture:

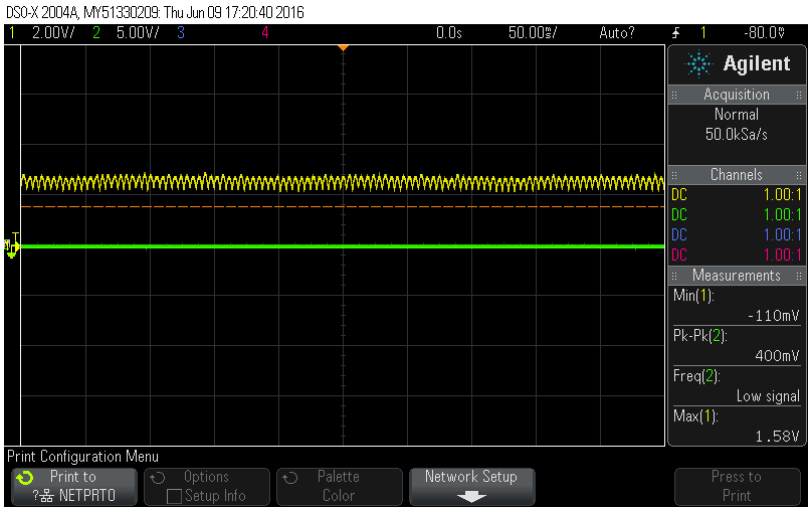

Figure 35: Snapshot of the rectifier output with no capacitator

When conducting tests, the rectifier was found to be working as expected. However, it was noticed that the voltage output from the rectifier, even though it remained relatively steady, showed small oscillations that are convenient to suppress. To do so, a capacitator was included in the original rectifying circuit, obtaining the following results:

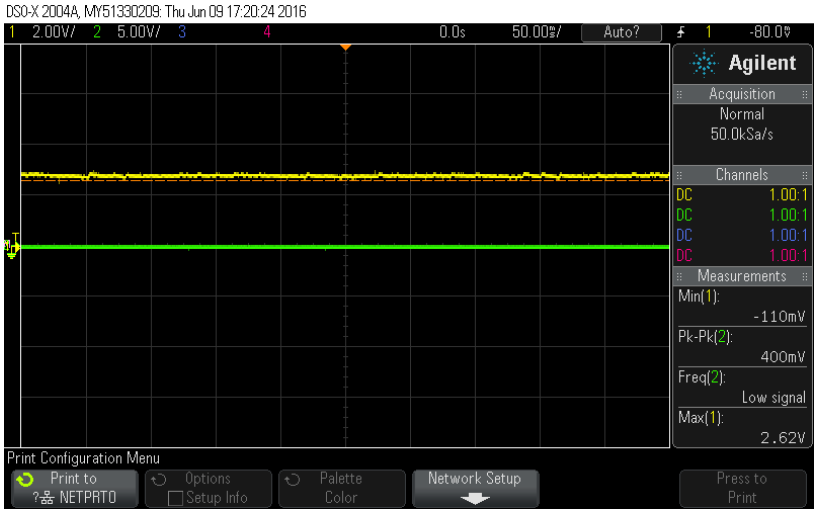

Figure 36: Snapshot of the rectifier output with capacitator

The capacitator used to fulfill this purpose has a capacitance of 330 nF. Using this capacitator is important because it will help improve the performance of the voltage regulator, and will reduce the effect that possible power drains from the turbine have in the electrical output.

3.3. Real life model testing

In this section, real-life experiments will be conducted to analyze the performance of the designed system. The tests to be carried out are:

- Cut-in flow test
- Variable resistive load test
- Variable flow test
- Battery charging test

For all the tests, a same set up will be used. The experimenting set up consists of a hose with a funnel that collects water from a tap. The tap makes possible to regulate the flow used during tests, and the funnel fills up, acting as a small reservoir that is continuously refilled. This flow goes down the hose and comes out inside the turbine's case, hitting the turbine and generating energy. The configuration of the set up can be seen in the following figure:

Figure 37: Set up used for the tests

At the end of the hose a nozzle is mounted. This part drastically modifies how the flow hits the turbine. When it is used the flow is strangled as a smaller cross-section area is available, but the water that reaches the runner is much more powerful, making it rotate faster than the water that has not been canalized through the nozzle would. The following figure shows the nozzle mounted into the turbine's case:

Figure 38: Nozzle used to inject the wáter onto the turbine

To obtain a better understanding of how the system functions when is subject to different conditions, the same experimenting set up will be used with two different heights. The first height used is 7.5 m above the ground, which is close to the height of a regular two-decked house. In the second place, the used height is 15.5 m. This height is used to simulate how the system behaves when it is used in a small building.

Unfortunately, it was not possible to obtain a flow meter to monitor the flow used during tests. To overcome this issue, every time flow had to be measured, a recipient with a scale was filled with the water from the hose and the time it took to fill to 1 L was recorded. The flow can be calculated then by just dividing the volume (1 L) by the recorded time. To reduce the error introduced by this way of measuring the flow, every measurement was done several times. By doing this, it is possible to calculate the average of the obtained results. The average of those results is closer to the actual value of the flow. Refer to the appendices to see the recipient that was used.

3.3.1. Cut-in flow test

The cut-in flow is the minimum flow at which the water turbine starts moving. Measuring the flow following the aforementioned procedure, the flows at which the turbine started rotating were:

Height (m)	*Flow (L/s)*
7.5	0.038
15.5	0.030

Table 6: Cut-in flow test results

3.3.2. Variable resistive load test

In this test, the main objective was to analyze how the performance of the system varies when loads of different magnitude is used. This test involves measuring the voltage across different resistors while a certain flow is being used to see the relation of flow, load and output power. The following diagram illustrates the circuit that was used for this test:

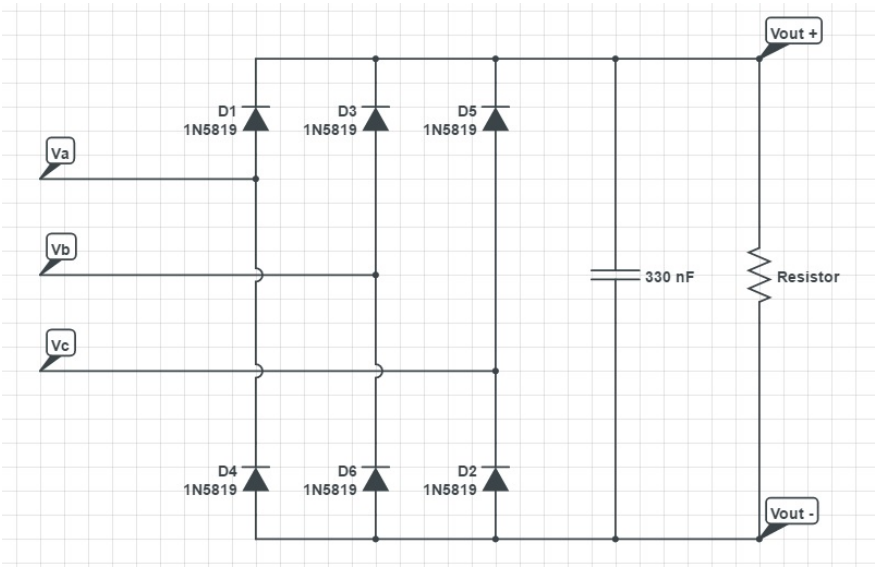

Figure 39: Diagram of the circuit used for tests

The following results were produced when the test was conducted using a 7.5 m height:

Flow (L/s)	*Load (Ω)*	*Voltage (V)*	*Current (mA)*	*Output power (W)*
0.149	1	0.16	160	0.0256
0.149	10	1.3	130	0.169
0.149	20	2.19	109.5	0.239805
0.149	50	3.69	73.8	0.272322
0.149	100	4.92	49.2	0.242064
0.149	200	5.89	29.45	0.1734605

Table 7: Variable load test results for h = 7.5 m

When testing the turbine from a height of 15.5 m, these results were produced:

Flow (L/s)	*Load (Ω)*	*Voltage (V)*	*Current (mA)*	*Output power (W)*
0.164	1	0.2	200	0.04
0.164	10	1.75	175	0.30625
0.164	20	2.98	149	0.44402
0.164	50	5.1	102	0.5202
0.164	100	6.8	68	0.4624
0.164	200	7.01	35.05	0.2457005

Table 8: Variable load test results for h = 15.5 m

The data is plotted in the following graphs to illustrate the relationship that exists between voltage and load, and between output power and load:

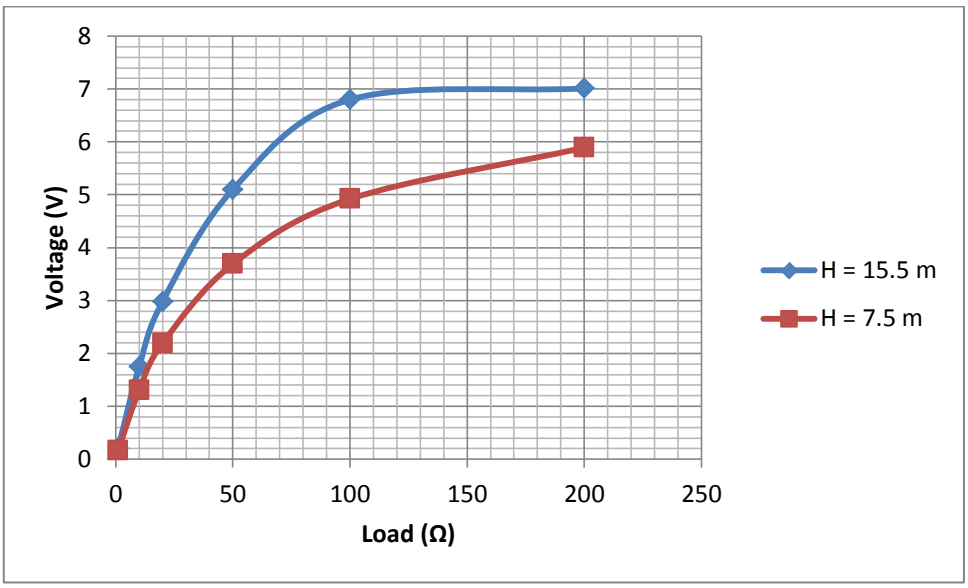

Figure 40: Voltage – load graph

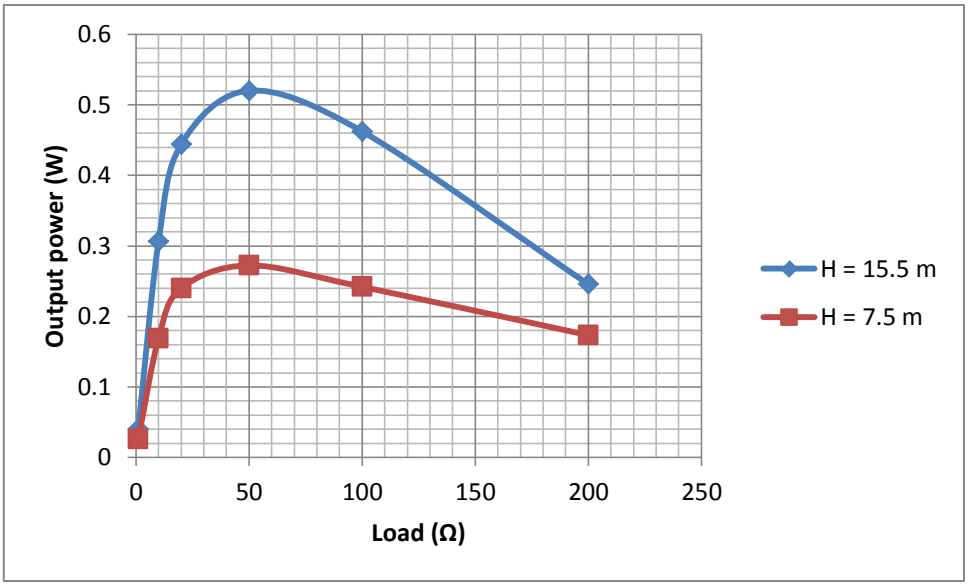

Figure 41: Output power – load graph

3.4.3. Variable flow test

The aim of this test is obtaining a curve that represents the flow versus voltage and flow versus power relationships, which is a common way of showing the performance of a water turbine. In this test, variable flows were used to operate the system while the same load was attached. The same circuit from the previous test was used for this one, but keeping the same load.

The following results were produced when the test was conducted using a 7.5 m height:

Flow (L/s)	*Load(Ω)*	*Voltage (V)*	*Output power (W)*
0.045	100	1.11	0.012321
0.106	100	3.5	0.1225
0.149	100	4.92	0.242064

Table 9: Variable flow test results for h = 7.5 m

When testing the turbine from a height of 15.5 m, these results were produced:

Flow (L/s)	*Load(Ω)*	*Voltage (V)*	*Output power (W)*
0.117	100	2.35	0.055225
0.137	100	2.9	0.0841
0.175	100	3.51	0.123201

Table 10: Variable flow test results for h = 15.5 m

The data is plotted in the following graphs to illustrate the relationship that exists between voltage and flow, and between output power and flow:

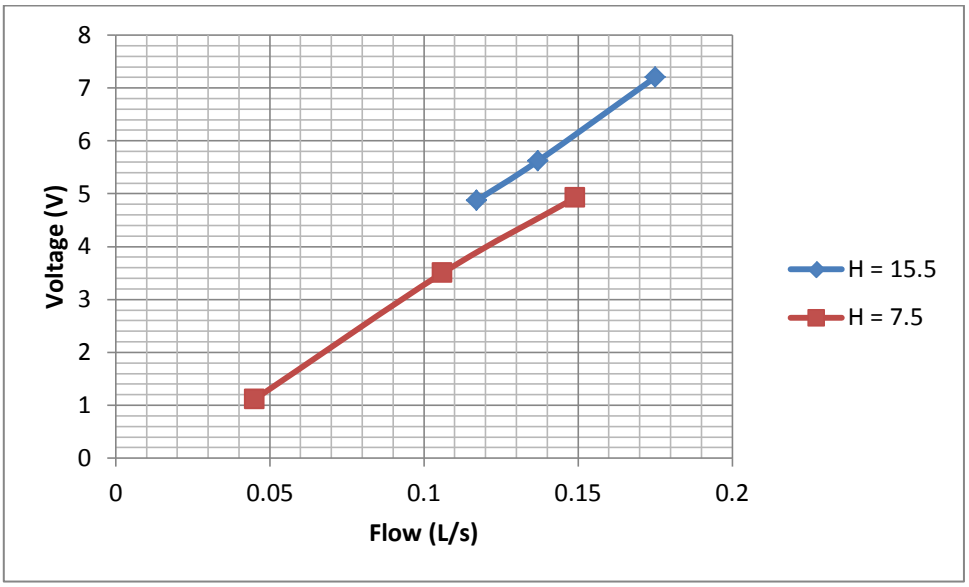

Figure 42: Voltage – flow graph

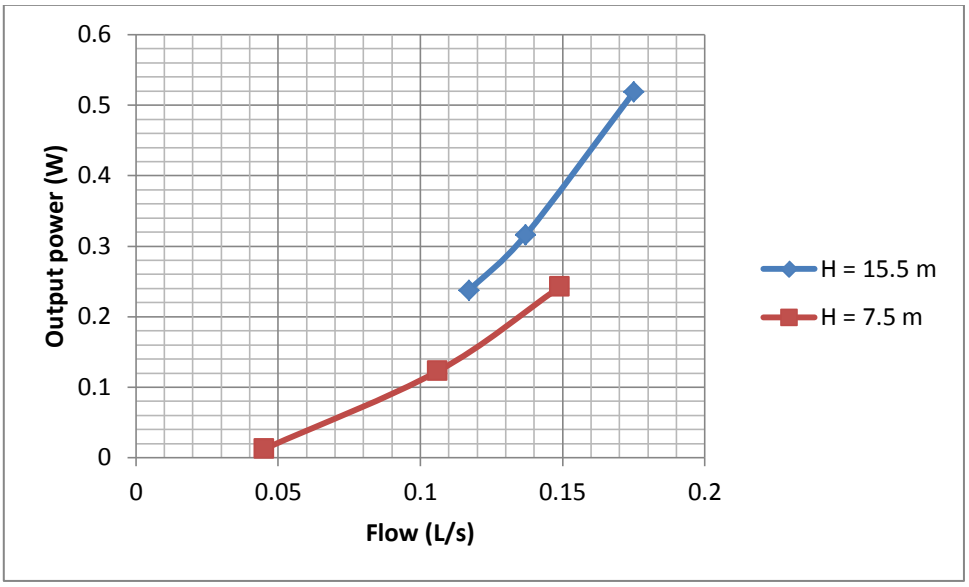

Figure 43: Output power – flow graph

3.4.4. Battery charging test

In order to test the actual utility of the proposed system, a test was conducted to see if the system was able to charge a battery. The battery used for this test was a discharged standard AA battery, connected to the output of the system. For this test, the final configuration of the power electronics was used, including the voltage regulator, as it can be seen in the following diagram:

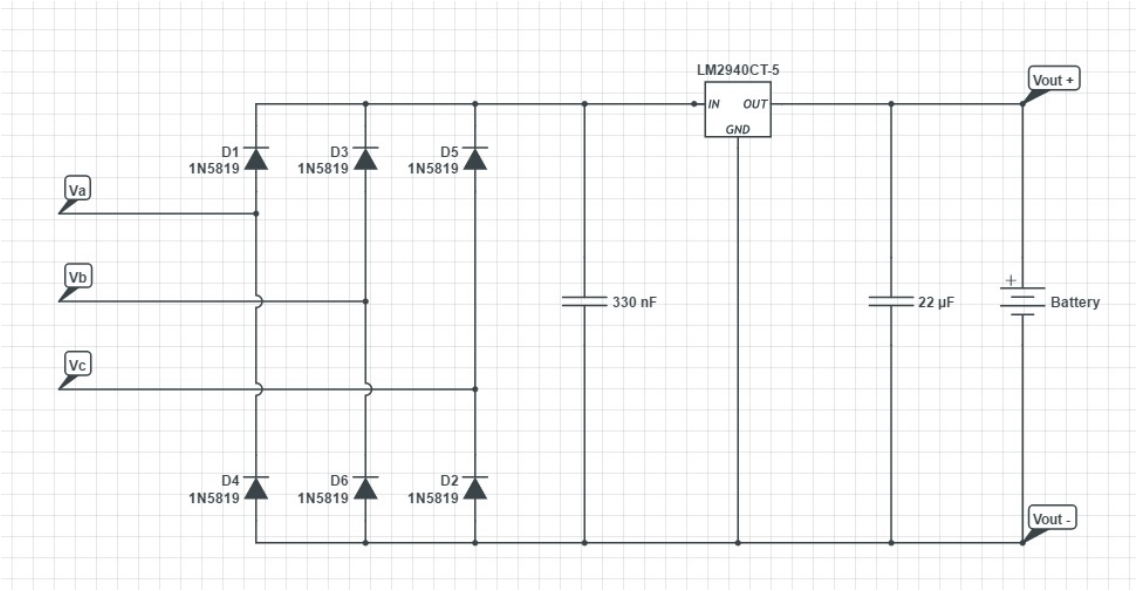

Figure 44: Diagram of the circuit used for the battery charging test

To determine whether the battery is charging or not, the multimeter was connected in series to measure any possible charging current.The tests from the two used heights produced the following results:

Height (m)	*Flow (L/s)*	*Initial voltage (V)*	*Final voltage (V)*	*Charging current (mA)*
7.5	0.155	0.81	1.01	69.5
15.5	0.149	0.83	1.05	68.7

Table 11: Battery charging test results

CHAPTER 4

RESULTS AND DISCUSSION

4. Results and discussion

The objective of this section is to analyze and interpret the results produced in the experimental investigation, giving them a meaning that helps elaborate conclusions about the performance of the real life model.

4.1. Electric generator testing

The results obtained from the voltage measurement tests indicate that the generator is able to provide enough voltage to undertake its task. However, the internal resistance of the generator seems higher than it should be for a generator this size, which can cause issues with the performance of the generator.

4.2. Rectifier testing

Observing the graphs obtained from the oscilloscope to analyze how the rectifier is working, it can be said that the rectifier works correctly. Moreover, the addition of the capacitator in the output of the rectifier has turned out to successfully remove the voltage oscillations that were present.

4.3. Cut-in flow test

Having a look at the minimum flow that was necessary to start moving the turbine, it can be said that in both cases it is a small flow. As expected, for the set up with a greater height, the minimum flow necessary to rotate the turbine was lower. The reason for this is that since in this case the water comes from a greater height, the available amount of energy for a same volume of water is greater. Therefore, a smaller amount of water is required to be flowing for the turbine to move.

4.4. Variable resistive load

When analyzing the results obtained in this test, it stands out the fact that the maximum power is obtained when the 50 Ω resistor is connected to the system. This load is the closest one to the internal resistance of the generator (35.6 Ω) from among the used ones, and that is the reason why the generated power reaches its maximum when this resistor is connected. For loads below or above 50 Ω, the output power decreases, although this decrease is faster if the resistance decreases.

The results obtained for the output power seem rather low for a system like the proposed one. This will be discussed in detail in following sections.

The curve representing the relationship between load and voltage shows that the greater the load, the higher is the voltage across the resistor. However, the generated voltage seems to be saturating for the larger loads, which means that the generator is reaching its maximum voltage generation capability. Therefore, if greater loads were used, the voltage across them would be expected to be higher, but the increment from one to another load would be smaller and smaller every time.

Although it has not been plotted, the current values seem to be quite low for the generator specifications, and they are higher with smaller loads.

4.5. Variable flow test

The results obtained in this test allowed an understanding of how the flow that is being used influences the performance of the turbine.

If we have a look at the voltage - flow graph, it can be seen that the voltage across the resistor is approximately a linear function of the input flow. This voltage across the resistor is also higher for the case where the greater height was used as the water coming from a greater height has a higher energy.

When analyzing the power – flow graph, however, the output power seems to be more of a slightly quadratic function of the flow that is reaching the turbine. Exactly as before, the obtained output power is higher for greater height case.

4.6. Battery charging test

In order to determine whether this test was successful or not, it is only necessary to have a look at the charging current that goes through the battery. Since the multimeter registered positive charging current of around 70 mA, it is clear that the charging is occurring, and therefore the charging capability of the system has been demonstrated.

Another indicator of the charging capability of the proposed system is the difference between the initial and final voltages across the battery once this is measured while it is disconnected from the hydropower system. In both cases, the final voltage is higher than the initial, proving the charging has taken place.

4.7. Efficiency

The efficiency is very important characteristic of systems like this one since it helps understand how much of the available energy can be transformed into usable energy. To analyze this parameter, the data set from the variable resistive load test will be used.

First of all, it necessary to calculate the available power that can be potentially transformed for every set up, because it depends on the flow that is reaching the turbine and the height from where the water starts going down. This calculation can be done using the expression $P_h = \rho Q g H$.

The following table shows the available power for each set up, assuming that 15% of that power is lost in the pipe due to narrowings, friction, etc.

Height (m)	*Flow (L/s)*	*Available power (W)*	*Losses (W)*	*Actual available power (W)*
7.5	0.149	10.9515	1.642725	9.308775
15.5	0.164	24.9116	3.73674	21.17486

Table 12: Available power for 7.5 m and 15.5 m set ups

The results obtained from comparing the available power and output power produced the following efficiency results for the 7.5 m set up:

Flow (L/s)	*Resistance (Ω)*	*Output power (W)*	*Efficiency*
0.149	1	0.0256	0.27500933
0.149	10	0.169	1.8154913
0.149	20	0.239805	2.5761177
0.149	50	0.272322	2.92543326
0.149	100	0.242064	2.60038512
0.149	200	0.1734605	1.86340845

Table 13: Efficiency results for h = 7.5 m

And for the 15.5 m case:

Flow (L/s)	*Resistance (Ω)*	*Output power (W)*	*Efficiency*
0.164	1	0.04	0.18890326
0.164	10	0.30625	1.44629055
0.164	20	0.44402	2.09692059
0.164	50	0.5202	2.45668684
0.164	100	0.4624	2.18372164
0.164	200	0.2457005	1.16034061

Table 14: Efficiency results for h = 15.5 m

The results have been plotted in the graph below for a better understanding:

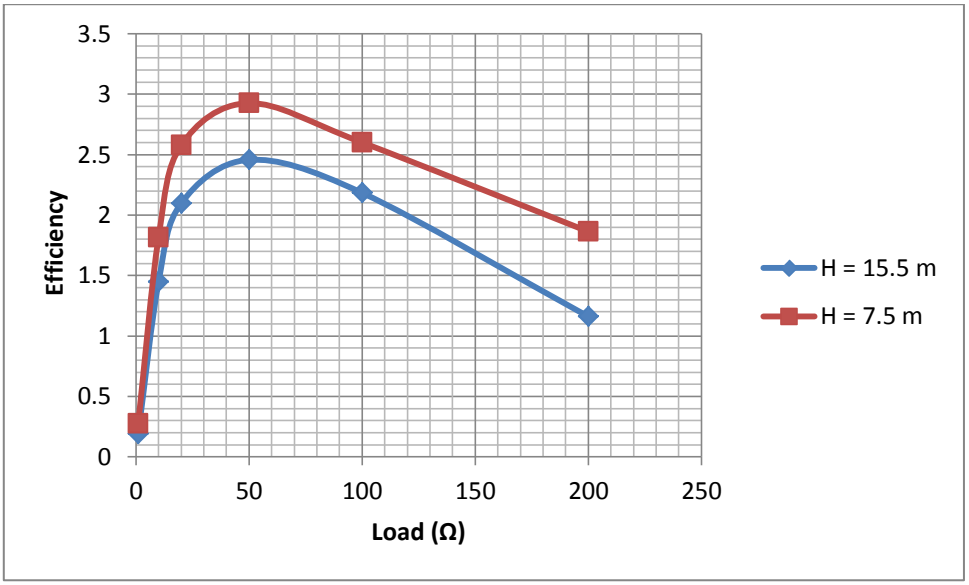

Figure 45: Efficiency – load graph

Analyzing the graph shows that the peak of efficiency is reached when the 50 Ω load is connected. The cause of this is that, from among all the tested resistors, the 50 Ω load is the one that generated the highest power. Also, it is important to note that the efficiency - load graphs have a shape that is similar to the power – load ones, since they are directly related. Another important characteristic that the graph reveals about the performance of the micro hydropower system is that efficiency is higher when the flow is lower.

Apart from that, what really stands out from this analysis is the low efficiency that the system has. Although the system is functional and able to charge a battery, it is not able to transform a large portion of the available energy. The reason why this happens is the high internal resistance of the generator, which creates high internal losses and limits the ability of the generator to provide the load with current, drastically reducing the output power. The performance of the general system could be greatly increased if this issue was addressed.

4.8. Feasibility study

In this section a simple analysis will be made to assess the feasibility of implementing a system like the proposed one. The following table shows the prices of all the components, being the total cost of the system $162.11, including an estimation of the installation costs that a project like this would incur:

Component	*Cost (AUS $)*
Pelton turbine	44.65
Electric generator	7.43
Bearing	19.95
Shaft coupling	7.23
Shaft (estimated)	18.3
Power electronics	14.55
Wood, bolts and others (estimated)	10
Installation costs (estimated)	40
	162.11

Table 15: Cost of components of the system

According to data provided by one of the main electric supply company of Australia, the price of every kWh of energy for a domestic installation is 23.331 cents (Origin, 2016). If we take the maximum output power of the micro hydropower system as a reference to make calculations, the time it would take to amortize the system would be:

$$\frac{162.11\ \$}{0.23331\ \frac{\$}{kWh}\cdot\frac{1\ kWh}{3.6\cdot 10^6\ J}\cdot 0.5202\ \frac{J}{s}} = 152.48\ years$$

Obviously this result is not satisfactory at all from the point of view of feasibility, and the reason is the low efficiency of the system, which does not exploit a large portion of the input power. If the efficiency was increased to 50% for the same case and the cost also increased $100 to fund the necessary modifications, the output power would increase to 10.585 W, which would yield the following result:

$$\frac{162.11\ \$ + 100\ \$}{0.23331\ \frac{\$}{kWh}\cdot\frac{1\ kWh}{3.6\cdot 10^6\ J}\cdot 10.585\ \frac{J}{s}} = 12.11\ years$$

Although this result is subject to change depending on the average rainfall of the area where the system is installed, it is much more reasonable and would definitely make the micro hydropower system viable as a product to be introduced in the market in regions where rainfall is abundant.

Even in places where rain is common, but not abundant, installing this system is a good idea since totally cost free energy would be obtained without harming the environment at all. In addition, no large works are needed to implement the system, and the investment required to do so is rather small.

CHAPTER 5

CONCLUSIONS AND RECOMMENDATIONS

5. Conclusion and recommendations

Throughout this capstone, the major principles of function in three-phase generators and water turbines have been reviewed. A prototype of a micro hydropower system was developed, built and tested to obtain a better understanding of this knowledge.

The results obtained from the several tests conducted allowed positive conclusions to be made about the performance of the system. Its capability to charge small batteries has been proved successful however the charging currents that the system is able to provide are quite low. Another negative aspect of the prototype is the low efficiency that it has, which poorly wastes the energy that is put into the micro hydropower system. Both of these are caused by the construction and characteristics of the electric generator: its internal resistance is a major drawback that adversely affects the performance of the system.

With a better generator and more refined design (which is relatively simple to accomplish with further time) the proposed micro hydropower system could not only greatly benefit in terms of output power and efficiency but it would also become a much more solid product in terms of feasibility.

A good substitute for the three-phase motor would be a DC generator of larger scale which would not only be able to satisfy the generation requirements but also would eliminate the need for the rectifier, increasing the overall efficiency of the system. The efficiency could also be increased by working at higher rotational speeds, where electrical machines reach their peak efficiency. Gears or some other sort of transmission system could be a way to achieve this.

Besides that, undertaking this project has provided a great deal of knowledge not strictly related to the topic of the capstone that will be very valuable in the development of an engineer, such as better time and stress management, dealing with suppliers and design and manufacturing approaches.

References

United Nations, “World Urbanization Prospects : The 2005 Revision”, viewed 18 April 2016, < http://www.un.org/esa/population/publications/WUP2005/2005wup.htm >

World Health Organization, “Urban population growth”, viewed 21 April 2016, < http://www.who.int/gho/urban_health/situation_trends/urban_population_growth_text/en/ >

A. A. Sallam and O. P. Malik, "Distributed generation," in *Electric Distribution Systems*, The Institute of Electrical and Electronics Engineers, Inc., 2011,

K. Narula, Y. Nagai and S. Pachauri, "The role of Decentralized Distributed Generation in achieving universal rural electrification in South Asia by 2030," *Energy Policy*, vol. 47, 2012.

Public Research Institute, “Types of turbine runners”, viewed 11 Arpil 2016, < http://www.publicresearchinstitute.org/Pages/hydroturbines/hydroturbines.html >

Renewables First UK, “Hydropower Turbines”, viewed 17 April 2016, < https://www.renewablesfirst.co.uk/hydropower/hydropower-turbines/ >

Unknown, “ Theoretical Background of Pelton Turbine”, viewed 23 April 2016, < https://el-umrah.onlinegroups.net/groups/te3218/files/f/19668-2010-11-03T071917Z/Pelton_theory.pdf >

J. Sabonnadière, "Small hydropower," in *Renewable Energies* Hoboken: John Wiley & Sons, Inc., 2009

Aguglie, “High efficiency pelton type water wheel 16 spoon”, viewed 2 May 2016, < http://www.ebay.com/itm/HIGH-EFFICIENCY-PELTON-TYPE-WATER-WHEEL-OF-WATER-MICRO-HYDRO-TURBINE-16-SPOON-/152130824677?hash=item236bb429e5:g:gykAAOxyaqlSTw8s >

A. E. Fitzgerald, C. Kingsley and S. D. Umans, *Electric Machinery*. London; New York: McGrawHill, 1992; 1990

Electrical riddles, viewed 3 May 2016, < http://electrical-riddles.com/topic.php?lang=en&cat=5&topic=289 >

Intech, viewed 5 May 2016, < http://www.intechopen.com/books/new-developments-in-renewable-energy/steady-state-modeling-of-three-phase-self-excited-induction-generator-under-unbalanced-balanced-cond >

Foshan, Gabodon Electronics, "'Three Phase AC Micro Brushless Wind Tube Generator Motor Hand-Cranked Generator'.", viewed 10 May 2016, < http://www.ebay.com/itm/Mini-Micro-Small-3-phase-Wind-Turbines-Hand-Alternator-Generator-3V-24v-12v-New-/322118779491?hash=item4affc68263:g:tcIAAOSwDV1XQuZQ >

N. Mohan, W. P. Robbins and T. M. Undeland, *Power Electronics :Converters, Applications, and Design*. Hoboken, NJ: John Wiley & Sons, 2003.

D. W. Novotny and T. A. Lipo, *Vector Control and Dynamics of AC Drives*. Oxford: Clarendon Press, 1996

Origin, "NSW RESIDENTIAL Energy Price Fact Sheet", viewed 7 June 2016, < https://www.originenergy.com.au/content/dam/origin/residential/docs/energy-price-fact-sheets/nsw/NSW_Electricity_Residential_AusGrid_Origin%20Supply.PDF >

Datasheets for electronics

Central Semiconductor Corp., "1N5819 Schottky barrier rectifier", viewed 16 June 2016,<http://www.jaycar.com.au/medias/sys_master/images/he3/h59/8832361103390/ZR1020-dataSheetMain.pdf >

National Semiconductor, " LM2940/LM2940C 1A Low Dropout Regulator", viewed 16 June 2016, < http://www.jaycar.com.au/medias/sys_master/images/h85/hdd/8832515440670/ZV1560-dataSheetMain.pdf >

Nationa Semiconductor, " LM78XX Series Voltage Regulators", viewed 16 June 2016, < http://www.jaycar.com.au/medias/sys_master/images/h29/he6/8832469237790/ZV1505-dataSheetMain.pdf >

APPENDICES

Appendix A: Multimeter

Manufacturer: Jaytech

Model: QM130

Appendix B: Oscilloscope

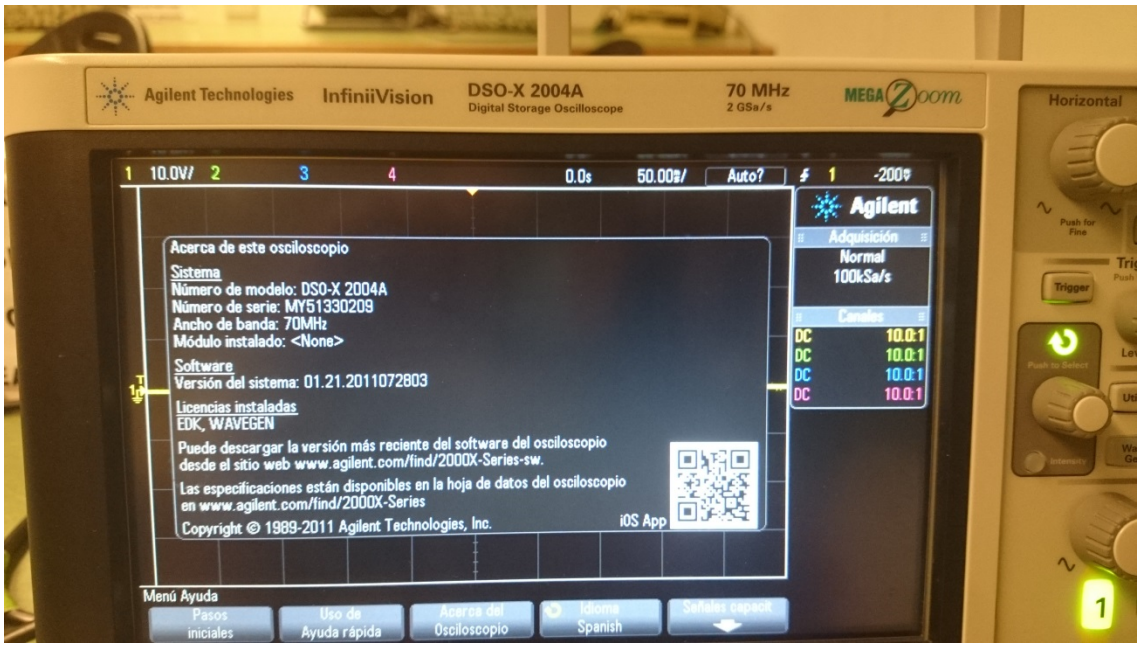

Manufacturer: Agilent Technologies

Model: InfiniiVision DSO-X 2004A

Appendix C: Hand drill

Manufacturer: Ryobi

Model: 4.0 Ah Lithium Battery 18 V

Appendix D: Volume measuring recipient

Manufacturer: Kmart

Maximum measurable volume: 1000 mL